

DTIC FILE COPY

# NAVSSSES

AD-A178 807

DTIC  
SELECTED  
APR 03 1987  
D

EXAMINATION OF COPPER-NICKEL  
SEAWATER PIPING REMOVED FROM  
USS VINCENNES (CG-49)

STATEMENT A  
public release  
unlimited

NAVAL SHIP SYSTEMS  
ENGINEERING STATION

PHILADELPHIA, PA 19112

87 3 17 015

**Best  
Available  
Copy**

2

DTIC  
ELECTE  
MAR 17 1987  
S D D

EXAMINATION OF COPPER-NICKEL  
SEAWATER PIPING REMOVED FROM  
USS VINCENNES (CG-49)  
DURING POST-SHAKEDOWN AVAILABILITY (PSA)

DISTRIBUTION STATEMENT A  
Approved for public release  
Distribution Unlimited

Approved for public release  
Distribution Unlimited

EXAMINATION OF COPPER-NICKEL SEAWATER  
PIPING REMOVED FROM USS VINCENNES (CG-49)  
DURING POST-SHAKEDOWN AVAILABILITY (PSA)

FINAL REPORT


BY

NORMAN J. CLAYTON

APPROVAL INFORMATION

SUBMITTED BY:

  
B. J. EICHINGER  
HEAD, MATERIALS BRANCH

  
S. TOLUTTA  
DIRECTOR, MEASUREMENTS & MATERIALS DEPARTMENT

APPROVED BY:

  
W. J. BOYLAN  
TECHNICAL DIRECTOR

Approved for public release; distribution unlimited.

UNCLASSIFIED

SECURITY CLASSIFICATION OF THIS PAGE

## REPORT DOCUMENTATION PAGE

1a. REPORT SECURITY CLASSIFICATION UNCLASSIFIED		1b. RESTRICTIVE MARKINGS N/A		
2a. SECURITY CLASSIFICATION AUTHORITY N/A		3. DISTRIBUTION / AVAILABILITY OF REPORT Approved for Public Release; Distribution Unlimited		
2b. DECLASSIFICATION / DOWNGRADING SCHEDULE N/A				
4. PERFORMING ORGANIZATION REPORT NUMBER(S)  PM-7378		5. MONITORING ORGANIZATION REPORT NUMBER(S)  N/A		
6a. NAME OF PERFORMING ORGANIZATION Naval Ship Systems Engineering Station	6b. OFFICE SYMBOL (If applicable) Code 053B	7a. NAME OF MONITORING ORGANIZATION  N/A		
6c. ADDRESS (City, State, and ZIP Code) Philadelphia, PA 19112-5083		7b. ADDRESS (City, State, and ZIP Code)  N/A		
9a. NAME OF FUNDING / SPONSORING ORGANIZATION Naval Sea Systems Command	8b. OFFICE SYMBOL (If applicable) PMS-400	9. PROCUREMENT INSTRUMENT IDENTIFICATION NUMBER  N/A		
8c. ADDRESS (City, State, and ZIP Code) Washington, DC 20362		10. SOURCE OF FUNDING NUMBERS		
		PROGRAM ELEMENT NO. N/A	PROJECT NO. N/A	
		TASK NO. N/A	WORK UNIT ACCESSION NO. N/A	
11. TITLE (Include Security Classification) Examination of Copper-Nickel Seawater Piping removed from USS VINCENNES (CG-49) during Post-Shakedown Availability (PSA)				
12. PERSONAL AUTHOR(S) Norman Clayton				
13a. TYPE OF REPORT Final	13b. TIME COVERED FROM 5/86 TO 11/86	14. DATE OF REPORT (Year, Month, Day) 1/28/87	15. PAGE COUNT 69	
16. SUPPLEMENTARY NOTATION  NONE				
17. COSATI CODES		18. SUBJECT TERMS (Continue on reverse if necessary and identify by block number) Copper-Nickel, Seawater Piping, Erosion Corrosion, Sulfide Corrosion, Turbulence, Microbiologically Induced Corrosion, Stress-enhanced corrosion.		
FIELD	GROUP			SUB-GROUP
11	06			
13	11			
19. ABSTRACT (Continue on reverse if necessary and identify by block number)  A failure analysis was conducted on several specimens of 90-10 copper-nickel seawater piping removed from USS VINCENNES (CG-49). Aspects such as erosion-corrosion, sulfide corrosion and microbiologically induced corrosion (MIC) were investigated. Erosion-corrosion due to turbulence was considered to be the main cause of damage to the piping. This type of attack was usually located within 12 inches downstream of a turbulence causing component such as an orifice or a butterfly valve. MIC and sulfide induced corrosion were both implicated in the analysis, but were not proven. Stress-enhanced corrosion was also implicated in the attack of fittings which were not in the fully annealed condition.				
20. DISTRIBUTION / AVAILABILITY OF ABSTRACT <input checked="" type="checkbox"/> UNCLASSIFIED/UNLIMITED <input type="checkbox"/> SAME AS RPT. <input type="checkbox"/> DTIC USERS		21. ABSTRACT SECURITY CLASSIFICATION UNCLASSIFIED		
22a. NAME OF RESPONSIBLE INDIVIDUAL N. Clayton		22b. TELEPHONE (Include Area Code) 215-897-7489	22c. OFFICE SYMBOL 053B	

DD FORM 1473, 24 MAR

33 APR edition may be used until exhausted.  
All other editions are obsolete

SECURITY CLASSIFICATION OF THIS PAGE

UNCLASSIFIED

**TABLE OF CONTENTS**

	<b><u>PAGE</u></b>
Introduction	1
Background	1
1. Cavitation	2
2. Erosion-Corrosion	2
a. Bulk Velocity	2
b. Turbulence	2
c. Entrained Particles	2
d. Chemical Corrodents in Fluid	3
e. Initial Film Condition	4
3. Microbiological Attack	4
4. Under-Deposit Corrosion	4
Procedure	4
Results	5
Sample A2	5
Sample A4	7
Sample A14	7
Sample A16	8
Sample B3	9
Sample B4	10
Sample B19	11
Sample B5	12
Sample C2	13
Sample C11	13
Sample D1	14
Sample D5	15
Sample G2	15
Sample G4	16
Sample J2	16
Check Valves	18
Discussion and Summary	18
References	20
Bibliography	21
Tables	23-31
Attachment (A) X-Ray Diffraction Results and Standards	
Attachment (B) Photographic Documentation	



Accession For	
NTIS CRA&I	<input checked="" type="checkbox"/>
DTIC TAB	<input type="checkbox"/>
Unannounced	<input type="checkbox"/>
Justification	
By	
Distribution /	
Availability Codes	
Dist	Availability for special
A-1	

SUBJECT: Examination of Copper-Nickel Seawater Piping Removed from  
USS VINCENNES (CG-49) During Post-Shakedown Availability (PSA).

## INTRODUCTION

The CG-47 class of ships, also known as the "AEGIS Cruisers", have experienced considerable accelerated deterioration of their seawater piping systems. The affected components have been almost exclusively 90-10 copper-nickel (90-10 CuNi) pipe, UNS alloy 70600 of specification MIL-P-16420. The problem has been common to every ship of the class so far. All of the ships have been built at Ingalls Shipbuilding Division (ISD) in Pascagoula, Mississippi; future ships will also be built at Bath Iron Works (BIW) in Bath, Maine. The problem has been most severe in piping which services electronics systems cooling, but has also been present to a lesser degree in seawater cooling piping for machinery systems such as air conditioning and air compressors. The extent of the piping leaks has been such that a three-day symposium was held solely to discuss the problem (reference (a)).

Reference (b) contains the results of failure analyses which were previously performed by NAVSSES on piping from the USS YORKTOWN (CG-48) and the USS VINCENNES (CG-49). The cause of attack on several of the samples was not positively identified in that investigation, but high seawater velocities and turbulent flow were considered to be the major influences on the deterioration. The influence of sulfide corrosion was implicated in some samples, but was not proven. Unfortunately, the origin and background of many of the samples analyzed had not been well documented, which prevented more definitive results. For this reason, when VINCENNES became available for a Post-Shakedown Availability (PSA), plans were made to open and inspect all of her seawater piping systems at locations which have historically been class problem areas. When badly deteriorated sections of piping were found, they were well documented and were returned to NAVSSES for examination. The piping returned to NAVSSES was generally thought to have had no more than nine months of service.

Fifteen pipe specimens were forwarded to NAVSSES for examination, along with two failed check valves. The specimens were removed from VINCENNES in March 1986, and were received by NAVSSES at the end of April. The samples are listed in Table I; the identifying characters correspond to codes developed for the open and inspect procedure, reference (c). The NAVSSES AEGIS Program Office provided funding for this study.

## BACKGROUND

The various potential causes of damage to 90-10 CuNi seawater piping have been extensively reviewed in references (a) and (b). A wealth of literature has been published on this subject, only a portion of which is reflected in the bibliography attached to this report. It is assumed that the readers of this report are somewhat familiar with the various damage modes, since most members of the Naval community concerned with this topic were present at the AEGIS Cruiser Seawater Corrosion Workshop held in May of 1986. For this reason, the modes of deterioration will only be briefly summarized herein without detailed references. The textbook evidence typically associated with each mechanism as found in failure analyses are also included. Keep in mind that textbook evidence is not always found in service failures, particularly where multiple mechanisms of attack are present. In addition, due to changes in the operation of a piping

system such as cycling between continuous use and no flow, different mechanisms of attack may have occurred at different times, with the most recent damage obliterating evidence of earlier damage.

1. Cavitation. Cavitation is caused by a sudden reduction of pressure in a flowing liquid, which in turn causes the formation and collapse of vapor bubbles on the metal's surface. The vapor bubbles can implode with enough force to remove protective surface films or even metal particles. The appearance of the attack is similar to very closely-spaced pitting, and the surface is usually very rough. Damaged piping from the AEGIS cruisers have not had any evidence of cavitation so far.

2. Erosion-Corrosion. In the simplest sense, erosion-corrosion is the rapid attack of a metal due to the movement of a corrosive fluid across the metal's surface. However, the number of factors which affect erosion-corrosion make the process far from simple. In the case of 90-10 CuNi in seawater, most of these factors involve damage to the protective cuprous oxide ( $\text{Cu}_2\text{O}$ ) film normally formed by the alloy. These factors are discussed below. Erosion-corrosion is generally characterized by smoothly grooved and gullied surfaces with rounded holes and undercut horseshoe-shaped pits, and usually exhibits a directional pattern. Modifications to this appearance by the various factors are also noted below.

a) Bulk Velocity: The bulk velocity reflects the design velocity of the piping system. It affects erosion via shear stresses imposed on the  $\text{Cu}_2\text{O}$  surface film on the pipe. The effect of bulk velocity and the magnitude of the shear stresses vary with the size of the pipe, due to changes in the fluid flow characteristics with inside diameter. The smaller the pipe size, the lower is the bulk velocity tolerable before the surface film is stripped off. Various velocity limit recommendations are presented in reference (a). It is generally agreed that the 15 feet per second (fps) limit currently imposed by reference (d) is too high for the commonly used pipe sizes between one and six inches. The appearance of erosion-corrosion due solely to excessive bulk fluid velocity should not vary from that described above, and the damage should be evident over the entire length of the piping. Piping affected by erosion-corrosion due to high bulk velocities would also not be expected to have any significant build up of deposits. Note that the effect of bulk velocity can not be totally separated from turbulence discussed below, since conditions which cause turbulence simply multiply the bulk velocity in local areas.

b) Turbulence: Turbulence is a disruption in flow which causes the fluid to come into more direct contact with the pipe's surface. This is usually accompanied by an increase in the local fluid velocity, which may be up to an order of magnitude greater than the bulk velocity. Flow disruptors which cause turbulence include foreign objects lodged in the pipe, sharp changes in fluid direction or in pipe cross-section, protrusions into the fluid such as sensors or weld beads, and ledges or gaps between mating components such as can occur at braze joints. Evidence of turbulence would be similar to general erosion-corrosion except that the damaged area is usually located just downstream or within an eddy of the turbulence promoter. As the fluid progresses down a length of straight pipe, the flow can again become laminar, and turbulence damage ceases.

c) Entrained Particles: Entrained abrasive particles, such as sand or silt, increase the erosion aspect of erosion-corrosion by mechanically removing protective films or surface metal. The particles can greatly accelerate erosion-corrosion attack caused by high bulk velocities or turbulence.



d) Chemical Corrodents in Fluid: Sulfide and ammonium ions are the two main species which have been found to increase the corrosion attack of 90-10 CuNi in seawater, with sulfide ions being the more damaging of the two. As little as 0.01 parts per million (ppm) sulfide has been found to greatly increase the corrosion rate of 90-10 CuNi. Both chemicals can occur in seawater as a result of sewage pollution of the water or from the decomposition of organic matter. Sulfides and high velocities or turbulence have been found to act synergistically to cause extremely damaging conditions. Laboratory studies and past Navy service experience indicate that a loose black film and circular, sharp-edged pits are characteristic of sulfide-induced corrosion. Another aspect of sulfide-induced corrosion is that tin bronze fittings are typically unaffected. X-ray diffraction deposit analyses are also performed in failure analyses where sulfide corrosion is suspected, but detection of sulfide compounds in deposits has been extremely difficult. Generally, indication of the element sulfur in the deposit by energy dispersive X-ray analysis (EDXA) has been used as evidence pointing to sulfide corrosion. This can not be used as absolute proof, since sulfur can also be present as sulfate, sulfite or other sulfur-bearing compounds. Ammonium ( $\text{NH}_4$ ) compounds would not be detected by EDXA since the elements nitrogen and hydrogen are not detectable by this method.

A detailed discussion of the effects of sulfide on the film chemistry of 90-10 CuNi will not be attempted in this report. The reader is referred to the papers in the bibliography for this information. However, a summary of film colors and analyses reported in the literature is presented in Table II. In this report, the term "sulfide" will be used to refer to both sulfide compounds and to sulfide ions in aqueous solutions.

Laboratory studies have shown that ferrous ions can inhibit the corrosive effects of sulfide. Therefore, the Navy has developed ferrous sulfate ( $\text{FeSO}_4$ ) injection systems. Since it was suspected that the AEGIS cruisers being built at ISD were experiencing sulfide attack, it was decided to test this system there. The systems only operate on the ships while they are at Ingalls. They are removed shortly before the last sea trials. In the case of USS VINCENNES, the system was back fitted at the end of January 1985 and removed at the end of April 1985.

There is no doubt that the presence of sulfide in seawater will increase the corrosion and pitting rate of 90-10 CuNi, and that the addition of ferrous ions to sulfide-containing water decreases this corrosion rate. This has been demonstrated in reproducible laboratory tests by various agencies, especially David Taylor Naval Ship Research and Development Center, Annapolis, MD. What is in question in the AEGIS cruiser problems is how much sulfide is present in the water and to what degree is it affecting the accelerated deterioration of the piping. For example, USS BUNKER HILL (CG-52) has had an  $\text{FeSO}_4$  injection system since it was built. However, during an inspection of her piping by NAVSSES 053B, the degree of attack observed was as severe as any on the other AEGIS cruisers. This was in spite of the fact that the red-brown film characteristic of a properly operating  $\text{FeSO}_4$  injection system covered the attacked areas.

e) Initial Film Condition: In addition to chemical contaminants in the seawater damaging the protective  $\text{Cu}_2\text{O}$  film, the quality of the initial film formed can also affect the erosion-corrosion resistance of 90-10 CuNi. However, this aspect is difficult to prove in a failure analysis, due to obliteration of the evidence by continued deterioration. Residual drawing lubricants left on the pipe prior to annealing heat treatment can become carbon deposits upon heating. These deposits are noble to CuNi, and cause galvanic corrosion. Lubricants and other contaminants which get on the pipe after heat treating can also cause damage by preventing good film adhesion or complete film formation. Water used to perform hydrostatic testing of newly installed piping systems is usually the first introduced into the pipe, and should be clean. This water should not be allowed to lie stagnant in the pipe after completion of the test, since it can then promote microbiological attack.

3. Microbiological Attack. Microbiological organisms can cause deterioration of 90-10 CuNi in at least two ways, each of which require the formation of a biofilm on the surface of the pipe. Sulfate-reducing bacteria (SRB) can use the sulfate which occurs naturally in seawater and turn it into corrosive sulfide compounds. However, this metabolic action requires anaerobic conditions. Colonies of iron and manganese reducing bacteria can form mound-like deposits on the pipe. Corrosion can then occur under these deposits due to acidic compounds secreted by the bacteria. Local anaerobic conditions can occur under these deposits, allowing SRB's to thrive and compound the corrosion problem. Mounds of deposits, and the detection of bacteria on the surface using a scanning electron microscope (SEM) are two clues which could point to microbiologically-induced corrosion (MIC). MIC may have a larger role in low flow rate or stagnant systems than in high flow rate systems, due to the association of deposits with this type of attack. However, biofilms formed on the pipe prior to service in flowing systems can be resistant to subsequent removal by the fluid.

4. Under-Deposit Corrosion. This variation of crevice corrosion has much in common with MIC. The distinction is made between deposits related to microbiological activity and those caused by mud, silt and organic matter in the pipe. As with MIC, this type of attack is normally associated with systems in which the flow rate is less than 3 fps, but can occur in more rapidly flowing systems if the deposits are adherent. An alloy such as 90-10 CuNi, which depends on an oxide film for corrosion protection, is particularly susceptible to crevice corrosion. This is because the protective film is usually damaged by high concentrations of chemical species which can occur under the deposits. The deposits inhibit diffusion of oxygen necessary to reform the protective film. Under-deposit corrosion can appear as pitting or as general surface corrosion.

#### PROCEDURE

Each of the pipe samples were visually inspected, split and photographically documented. Attachment (B) contains the photographic figures referenced in this report. Figures 1 to 16 show the macroscopic features of each specimen. After splitting, additional visual examinations were performed with the aid of a stereo-microscope. Narrative descriptions of the attack characteristics and deposits are contained in the following section of the report.

Samples for material chemistry identification by EDXA were removed from each of the piping assemblies. The results are shown in Table III. Table III also lists the minimum specified flow rates for each system, the nominal

specification wall thicknesses based on pipe size, the minimum measured wall thicknesses and a summary of what is considered to be the primary cause of deterioration of each pipe sample.

Deposits were collected from many of the samples for analysis by X-ray diffraction and EDXA. The results of these analyses are summarized in Table IV. No sulfide, sulfate or ammonium compounds were detected, although trace amounts of sulfur were identified by EDXA. The specimens were collected by scraping large areas of a component half down to bare metal using a clean stainless steel spatula. This has probably resulted in artificially high EDXA results for iron. The X-ray diffraction spectra are provided in Attachment (A). The diffraction standard for lepidocrocite ( $\text{FeO}\cdot\text{OH}$ , the main constituent of the film typically associated with ferrous sulfate injection) has also been included in Attachment (A). There are many crystallographic forms of the various copper sulfides. Standards of several of these compounds may also be found in Attachment (A).

The results of metallographic examinations and hardness tests are included in the narrative of the next section. The hardness tests were performed using a Knoop microhardness indenter with a 500 gram load, and using a Rockwell superficial hardness tester on the 30-T scale. The results have been converted to their approximate Rockwell B-scale (RB) values for a more common reference. Due to variations in different hardness conversion tables for non-ferrous alloys, the values reported should not be interpreted as absolute values, and are intended for comparison purposes only. For reference, 90-10 CuNi tube in the annealed condition has a typical hardness level of RB15-25. In the lightly drawn/cold worked condition, the typical hardness is RB60-80. Reference (e) is the drawing which governs Class 200 90-10 CuNi fittings, which includes concentric reducers and 90° elbows. Note 6 of reference (e) is titled "Hardness", and states that finished fittings shall be furnished in the fully annealed condition. However, no actual hardness limits are given.

Pipe halves from samples A4, G4 and J2 were forwarded to Dr. Brenda Little of the Naval Oceanographic Research and Development Activity (NORDA) for examination for possible evidence of MIC. Dr. Little also performed EDXA of deposits from these specimens, and provided photomicrographs displaying colonies of microorganisms on two of the samples surfaces. The results of this work are described in the next section, and were summarized in reference (f).

## RESULTS

Sample A2. Figure 1a shows the arrangement of the piping system in the area of this sample. The sample was 11 inches long and was installed on the ship in the vertical plane. The rotational orientation of the sample relative to the 90° elbow from the flex hose dogleg is not known. The flex hose fitting was one of the "Aeroquip" fittings which are known to have a subsize outlet. In reference (a), minimum velocities in excess of 19 fps were estimated at the outlet of these fittings in the AEGIS piping systems. The joint fit-up at the braze and welds was fairly good, with no weld bead protrusions into the flow path. The pipe-reducer weld only penetrated to the inner diameter (ID) in places. The reducer-flange weld did not penetrate to the ID.

Figures 1b, c and d show the interior of the pipe after splitting. The

pipe had a hole in it at the inlet end immediately beyond the end of the brazed flange. The area surrounding the hole was bright yellow. It is quite possible that the pipe may have been aligned so that the brunt of the flow out of the elbow impinged on this side of the pipe. The most severe attack was on the same side of the pipe as the hole, and on the section of pipe enclosed by the flange. A multi-layered, multi-colored deposit was present on the pipe and the reducer. The topmost layer on the pipe was green/gray/brown, shifting to brown/gold on the reducer. A black layer of deposit was under the top layer, and a gold/brown layer was closest to the metal's surface. The black deposits were loose as compared to the other ones, and were generally associated with the deeper areas of attack. There was minor attack of the pipe-reducer weld, but the heat affected zone (HAZ), a quarter-inch to either side, was unaffected. There was also no sign of attack in the one-inch wide HAZ of the reducer-flange weld. This can be seen in Figure 1d. Both flanges were also unaffected. There was bright, iridescent metal under all of the deposits, indicating recent active corrosion. The undersides of the deposits were either purple/maroon or black. There was no sign of cavitation damage.

As shown in Table III, there were no discrepancies in the component chemistries. Although no sulfur or sulfides were detected in the deposits collected for X-ray diffraction, Table IV shows that trace quantities of sulfur were detected in EDXA performed on the surfaces of black deposits. This finding, in combination with the looseness of the black deposits and the general attack of the entire surfaces of the pipe and reducer, implicates sulfide corrosion as a factor in this failure. However, the gross amount of metal removal in a relatively short period of time suggests that the sulfide corrosion mechanism only served to accelerate deterioration which was largely caused by erosion-corrosion due to high flow rates and turbulence.

There were no microstructural abnormalities in either the pipe or the reducer. The pipe had a hardness level of RB23-44 except at the braze and weld HAZ's, where the range was RB13-25. This softening in the HAZ is considered normal. There was no grain boundary damage or other signs of overheating during brazing. At low magnifications, the attack on the pipe's surface appeared smooth, and was slightly undercut in the direction of flow in a few places. The attacked surfaces were noticeably rougher at higher magnifications, indicating some under-deposit corrosion. The attack was independent of grain boundaries. There was a very narrow region of grain growth at the pipe-reducer weld, indicating good heat input control. The attacked surface of the reducer was generally smooth with no undercutting. The hardness of the reducer ranged from RB17 at the HAZ of the weld to the pipe, to RB48-74 out of the HAZ. This indicates that the reducer was not in the fully annealed condition. The wide variation in hardness is due to the cold work required to form the reducer. This raises the possibility of stress-enhanced corrosion as a factor in the damage to this reducer. This mechanism is described in more detail for specimen J2 and in the Discussion section of the report.

In summary, the failure of the pipe is considered to be largely the result of erosion-corrosion caused by high flow rates and turbulence coming out of the 90° elbow upstream. Under-deposit corrosion was also occurring further downstream on the pipe and the reducer, but this attack was less severe. Sulfide corrosion is also likely to have contributed to the damage on both components. Pitting of the reducer may have been enhanced by residual stresses from its fabrication.

Sample A4. Figure 2a shows the arrangement of the piping around this 23-inch long sample. The sample was oriented horizontally. The 90° flex hose elbow upstream of the pipe was one of the flow-constricting Aeroquip fittings which produce above-design velocities. The joint fit-up of the two brazed flanges was good, with little or no gap.

Figures 2b and c show the sample after splitting. Two large areas of the pipe were eroded completely away at the inlet end within the flange sleeve. This can be seen in Figure 2c. The two damaged areas were about 180° apart. Both the top and bottom halves of the pipe were affected. These areas had been repaired by ship's force. There was light to moderate pitting on the top half of the pipe, which extended more than halfway down the pipe from the inlet. The bottom half of the pipe was covered with a light green film where seawater probably evaporated during the last down time of the system. However, there was no significant attack of the bottom half other than the areas at the inlet. The rest of the pipe was covered with a film that was mainly black, with green/brown spots in it. There was evidence of active corrosion under loose deposits, but this attack was very light. The pits on the pipe had rounded bottoms. There was no evidence of cavitation.

Table III shows that the pipe and flange materials were normal. Table IV shows that traces of sulfur were found by EDXA of deposits from the pipe, but that no sulfides or other unusual compounds were detected by X-ray diffraction. The outlet end of the top half of this sample was sent to NORDA for examination for MIC. NORDA was unable to verify whether MIC had occurred, but did find that filamentous microorganisms were colonizing the surface of the pipe. As shown in Table IV, EDXA of the surfaces of deposits from the pipe produced similar results to work performed at NAVSSES, confirming that sulfur was present.

The wall thickness of the pipe ranged from zero at the inlet to 0.099" - 0.104" at non-attacked areas at mid-pipe. The wall thickness was reduced to 0.085" in some of the small pits present on the top half of the pipe. The microstructure of the pipe was normal and uniform. The surface of the pipe was smooth and rounded in the attacked areas, suggesting erosion-corrosion caused by turbulence and high flow; however, there was no distinct undercutting. The attack was independent of grain boundaries, and there was no sign of overheating at the braze joints. Hardness tests performed on specimens from this sample produced erratic results, ranging from RB 17-50 in areas away from HAZ's, and RB 26-42 in the area of the inlet braze HAZ.

In summary, the localized attack at the inlet end of sample A4 is attributed to erosion-corrosion caused by turbulence from the upstream elbow. There was also light under-deposit corrosion on the remainder of the pipe. This may have been enhanced by the presence of sulfide or microorganisms, but these factors could not be proven.

Sample A14. This 4.5" long sample is shown in Figure 3. The sample was positioned vertically in service. The weld joints on this sample were fairly sloppy. Weld metal droplets protruded into the flow path around much of the circumference at the outlet end of the reducer. The largest protrusion measured approximately 3/16". There was also about a 1/8" gap at the flange-reducer joint.

In spite of the relatively large metal droplets in the flow path, there was little or no attack of the pipe immediately downstream of the weld. Deterioration of this sample was on one side of the reducer at the inlet end. The reducer metal was completely removed at its inlet edge, and was worn down to a feathered, knife-like edge. The exposed lip of the flange had also experienced some roughening in this area. There was no loose deposit on any area of the sample. In the area of the reducer with the most metal loss, the surface was wavy and smooth, with rounded depressions and a dull gold/olive-green film. Immediately surrounding this area, the reducer's surface was very rough, with the appearance of closely-grouped light pitting. This area and the rest of the sample had a fairly uniform gold/brown film on it. The above evidence indicates that cavitation, and erosion-corrosion due to impingement downstream of the pump caused the damage. It is noted that the 2.5" reducer inlet downstream of the AEGIS pump is considered a poor design and will probably be a chronic problem area on the AEGIS cruisers. The use of a pump with a 3" discharge could help to minimize the erosion-corrosion aspects of the attack, but may cause worse cavitation by increasing the pressure drop at this location.

The materials of sample A14 were all 90-10 CuNi with correct iron contents. The film scraped from the sample was analyzed using EDXA. The results are given in Table IV, and show that there was no sulfur in the film.

The wall thickness of the reducer in non-attacked areas of the bell was 0.098"-0.102". The wall thickness of the nipple downstream of the reducer was 0.098"-0.101". Hardness tests of the reducer, welds and HAZ's in various locations did not produce consistent results. The microstructure of the reducer was normal and uniform. There was limited grain growth at the HAZ's of the welds, indicating low heat input. There was some undercutting of the reducer at the edge of the heavily attacked area. There was also some undercutting immediately in front of the protruding weld droplets on the reducer. This is shown in Figure 17. This may have been an effect of back-eddying of the flow at this location. The attack was independent of grain boundaries in the metal.

In summary, the damage to sample A14 was caused by localized erosion-corrosion due to impingement downstream of the pump, and by cavitation occurring on one side of the reducer.

Sample A16. This sample is shown in Figure 14. The inlet end of the sample was horizontal, and had been located immediately downstream of a butterfly valve. The pipe then curved upward to meet a strainer.

There was a large hole on one side of this sample as shown in Figure 14c. This hole was surrounded by deep pits, and the flange was damaged on this side as well. There was a light blue/green film over the bottom portion of the pipe, corresponding to where seawater would have laid during lay-up periods. The remaining surface of the pipe exhibited a "textbook" example of the uniform gold/brown film generally associated with good Cu<sub>2</sub>O formation. There was no loose deposit anywhere on the sample.

The pipe and flange had acceptable compositions. The microstructures were also normal. Sections through the pits showed that they had undercutting in the direction of flow. No hardness tests were performed on this sample.

The damage on this sample is attributed to erosion-corrosion caused by seawater impinging on the side wall of the pipe as it was redirected by the butterfly valve.

Sample B3. Photographs of this 16" long sample are presented in Figure 4. This sample was positioned vertically on the ship. In reference (a), the AEGIS cooler upstream of this sample was reported to have an orifice plate near its discharge. The joint fit-ups on this sample were good, with no gaps or protruding weld metal droplets. The reducer-flange weld did not penetrate to the ID. The reducer-pipe weld barely penetrated to the ID in a couple of locations.

As shown in Figure 4b, the attack of the reducer was unevenly distributed. The metal was either completely unaffected, or had large areas of severe damage. There was no pattern to the location of this damage other than the fact that the deepest attack was in the belled central portion of the reducer. The attack occurred both within and away from the HAZ's of the reducer welds. Areas which had not been affected were covered with an adherent, thin orange/brown film. The pitted areas in the reducer were covered with a black/brown film. As shown in Figure 18, there were also many smaller round pits within the large attacked areas of the reducer. This type of damage is unique to this sample. (The scrape-marks on either side of the pitted area are a result of collecting deposits for analysis.)

There was only mild spotty attack of the pipe for 6" back from the reducer-pipe weld. As with the reducer, unaffected areas have a thin, uniform orange/brown film. Anywhere this film was damaged, a black deposit and general corrosion were present. This is illustrated in Figure 4c and Figure 19. The last 4" of the pipe up to the outlet flange was completely covered with this black deposit, and was generally deteriorated around the entire circumference. The black scale was fairly loose, and there was evidence of active corrosion under it.

There was nothing unusual in the chemical compositions of the components which made up this sample. Deposits were collected separately from the reducer and the outlet end of the pipe. Table IV shows that no sulfide, ammonium or other corrosive compounds were detected. However, traces of sulfur were detected on the surfaces of both black and orange/brown flakes of deposits. SEM photomicrographs of the surfaces to these deposits are shown in Figures 20 and 21. It is interesting to note that the EDXA spectra from these deposits were very similar, but that the color, adhesion and topography of the deposits were radically different. It is suggested that the sulfur in the black deposit was present as sulfide in quantities below the limit of detection of the x-ray equipment, whereas the sulfur in the orange/brown deposit was present as a sulfate. The mudlike cracking of the black deposit shown in Figure 21 probably occurred upon drying.

The microstructures of the reducer and pipe were normal, with only a narrow region of grain growth in the HAZ of the weld joining the two. Pits in the reducer were undercut in the direction of flow. This is shown in Figure 22, which shows a couple of the smaller pits located within one of the large attacked areas. The pits in the reducer were rounded and smooth. The corrosion of the pipe under the black deposits had a rough appearance. The attack of both the pipe and the reducer was independent of grain boundaries. The hardness level of the reducer ranged from RB48-67, and was RB30-33 in the

HAZ of the pipe weld. As with sample A2, the reducer was not in the fully annealed condition. The pipe had a baseline hardness of RB29-38, and a weld HAZ hardness of RB17-25.

Sulfide contamination is thought to have had a predominant role in the deterioration of this sample. The cause of the damage to the reducer is thought to be due to erosion-corrosion induced by turbulence out of the AEGIS cooler which only affected areas where sulfide broke down the protective film on the reducer. Stress-enhanced corrosion may also have been a factor in the pitting of the reducer, as described in the Discussion section of the report. The attack of the pipe is considered to be due to erosion-corrosion induced by the combination of a marginally high bulk velocity and the presence of sulfide.

Sample B4. The configuration of this sample is shown in Figure 5a. The sample is actually made up of the two spool pieces (B4.1 and B4.2) which surrounded an in-line flowmeter (FM1). This 3-piece assembly was replaced with a single length of pipe during the PSA. Not shown in Figure 5a is the fact that a 90° elbow coupling from one of the Aeroquip flex hoses was located immediately upstream of specimen B4.2. The four flanges on B4.1 and B4.2 were all brazed. There were minimal or no gaps at the joints. These samples were arranged horizontally on the ship.

Views of the inlet and outlet ends of B4.1 are shown in Figures 5b and 5c respectively. Sample B4.1 had light attack along the first 8" of its inlet end. The entire circumference of the pipe was affected. The film over this area ranged from orange/brown right at the inlet end, to darker shades of brown for most of the remaining length of the pipe. The inlet attack was smooth and there was no loose deposit in this area. There was loose deposit in the central portion of the pipe with signs of corrosion underneath, but the depth of attack was insignificant. The outlet end of this sample is where the real damage occurred, as shown in Figure 5c. This area had been repaired by ship's force, which accounts for the discoloration surrounding the hole. This damage was very rough, and was not oriented in the direction of flow. It was also predominantly located in the bottom half of the pipe.

Attack of the outlet end of a pipe is contrary to what is normally observed. In this case, the attack is attributed to the internal parts of flow meter FM1 coming loose and sliding down the pipe until they hit the orifice plate at the outlet end of B4.1. These parts would sit in the bottom of the pipe and would create local turbulence. Notes from the shipyard at the time of opening the pipe for the PSA stated that the internals of the flow meter were missing. However, a set of these parts was found on the deck in the compartment where this piping was located. These parts are shown in Figures 16a and 16b. The parts were probably removed from B4.1 by ship's force when they repaired the pipe.

As shown in Table III, there was nothing unusual about the compositions of the compounds of B4.1. No deposit analyses were performed on this sample. B4.1 had a uniform, normal microstructure with a baseline hardness of RB27-46. There were no signs of overheating or other microstructural changes in the HAZ's of the brazes. The inlet end attack was smooth and rounded in cross-section, and was independent of grain boundaries. This light attack is considered to be due to erosion-corrosion caused by turbulence downstream of the flow meter while it was still intact. A section taken through the central portion of the pipe had light uniform corrosion attributed to under-



deposit corrosion. A longitudinal section through the damage at the outlet end had undercutting in both directions, indicative of eddying of the seawater around an obstruction.

The entire pipe of B4.2 had been badly damaged. A portion of the damage is shown in Figure 5d. There was insignificant attack of the flanges. There was a band of fairly adherent black film around the center of the pipe, which had white splotches on it. Figure 23 shows the surface of the pipe under a flake of loose black deposit. The pipe had a brown/gold film on either end. The attack was equally severe in all areas of the pipe. A thick layer of deposit had collected at the outlet end of the pipe against the flange, and the pipe had been perforated in a few areas under this deposit. The underside of this deposit was maroon/purple.

The compositions of the components of B4.2 were normal. Analysis of the white splotches on the pipe showed that they mainly contained titanium. These stains are considered to have come from white marking fluid, since titanium dioxide ( $TiO_2$ ) is a widely used white pigment. They did not affect the attack of the pipe, and probably got on the pipe after it had been removed. No sulfides were detected in the deposits by X-ray diffraction, and no sulfur was found in EDXA of the powdered X-ray specimen. However, Table IV shows that a trace amount of sulfur was detected by EDXA of a cross-section of the deposit which had collected at the outlet flange. The deposit cross-section is shown in Figure 24 and the accompanying EDXA spectrum is shown in Figure 25. The maroon undersides of some deposits were also examined. These areas had a part globular, part crystalline appearance. Figure 26 shows the typical appearance of the maroon deposit undersides found throughout this investigation. This figure is actually from sample G2.

Metallographic examinations and hardness testing showed that sample B4.2 had a normal microstructure with a baseline hardness of RB27-47. Figure 27 shows an example of what is considered to be a normal microstructure as referenced throughout this report. These are roughly equally sized grains with a grain size of 0.030" to 0.040". Sections of B4.2 had rough corroded surfaces under the deposits. Although Figure 23 appears to indicate that the attack had a somewhat intergranular nature, no grain boundary dependence was found metallographically. In the outlet braze HAZ, a very low hardness at the bottom of the RB scale was measured. There had also been a slight amount of grain growth. No other microstructural changes were observed.

In summary, the cause of attack on sample B4.2 is uncertain. Under-deposit corrosion, turbulence out of the Aeroquip fitting and sulfide corrosion may all have been simultaneously acting on this piece. The severity of the damage over the entire length and circumference of the pipe also suggests that the initial protective film either never formed, or had been contaminated as discussed in the background of the report.

Sample B19. Figure 5a shows the arrangement of sample B19, and Figures 5e and 5f show as-split views of the inlet and outlet ends of this sample, respectively. This sample was positioned horizontally on the ship. The flange joint fit-ups were good, and there were no significant weld bead droplets protruding into the pipe.

As shown in Figure 5e, there was severe attack of the inlet end of the pipe in a well defined line about 1.5" back from the flange. This attack affected the entire circumference of the pipe. In the location shown in Figure 5e, the attack perforated the pipe, which required repair by ship's force. Deep, sharp-edged pits were scattered within 5" downstream of this line of attack, and were predominantly located in the bottom half of the pipe. The only other area of damage on this sample was between the two welds at the outlet end of the pipe. This shallow damage can be seen in the upper portion of Figure 5f. There was a gold/brown film at the inlet end of the pipe between the flange and the line of attack. Downstream of the attack, the pipe had a thin, uniform black film for the rest of its length, except for small areas surrounding welds in the pipe, which were gold/brown.

The compositions of the piping components were normal. Analysis of the black deposits at the inlet end of the pipe by X-ray diffraction did not reveal any sulfide, but EDXA of the powdered X-ray sample detected a trace amount of sulfur. The sharp-edged isolated nature of the pits downstream of the line of attack indicates that sulfide-induced corrosion may have been acting. The deepest of these pits had reduced the wall thickness to 0.015"; the pipe was 0.085" thick immediately adjacent to this pit.

The microstructure of this pipe was uniform and normal in both attacked and non-attacked areas. Sections through single pits showed that they were smooth and rounded with no undercutting. Sections through the line of attack showed that it was undercut in the direction of flow. The pipe had a baseline hardness of RB38-48.

In summary, the line of attack around the inlet end of this sample is attributed to local turbulence downstream of the orifice plate. Sulfide corrosion may have enhanced this damage, and is thought to be the primary cause of the isolated pits further downstream.

Sample B5. This sample is shown in Figure 6. It was positioned vertically in the ship, except for the inlet end, which bent into the horizontal plane to meet the butterfly valve. The two flanges on this piece were welded on, and there were two partial penetration welds in the piping. The joint fit-ups were good and there were no weld droplet protrusions.

The only damage in this entire 5 foot long piece consisted of two local pits on one side of the inlet end as shown in Figure 6c. One of these pits required repair by ship's force, as it had perforated the pipe. There was a gold/brown film in each of the welds' HAZ's. The remainder of the pipe was covered with a black/brown/gray film with spots of green in it.

No deposit analyses or hardness tests were performed on this sample. EDXA of the material compositions produced normal results as shown in Table III. The piping had a normal microstructure, with narrow regions of grain growth at weld HAZ's. A section through one of the pits showed that it had a generally rounded and smooth profile with no undercutting. The wall thickness was 0.095" next to this pit, and was 0.010" at the bottom of the pit.

This damage is attributed to erosion-corrosion caused by impingement of the seawater on the side of the pipe. The seawater was probably directed against the side of the pipe by the butterfly valve.

Sample C2. Figure 7a shows the configuration of this sample, and Figure 7b shows one half of the sample after splitting. This piping was vertically positioned on the ship. All of the joints on this sample were made by welds. The flange-reducer joint was slightly offset in a few locations around the circumference, resulting in small gaps or ledges as shown in Figure 7b. However, this did not affect the reducer, which was uniformly attacked all of the way around. Similarly, the joint between the reducer and the short pipe bend also had a ledge in some locations, which did not cause any attack of the pipe. The weld between the pipe bend and the short straight nipple was the only full penetration weld. Weld metal droplets protruded slightly into the pipe (less than 1/8"), but there was no downstream damage to the nipple.

The damage to the reducer was greatest in the bell section. As shown in Table III, up to 0.050" of metal had been removed in the deepest pit. There was also light attack of the reducer where it straightened out to meet the pipe bend. The entire sample was covered with a uniform gold/brown film except for the outlet end, which was darkened as a result of heating the braze joint during PSA to remove the flex hose coupling. The gold/brown film covered attacked and non-attacked surfaces of the piping equally. The metal beneath loose flakes of this deposit was bright, iridescent and grainy, suggesting recent active corrosion. The underside of this deposit also had a maroon/purple color, indicative of redeposited copper as noted in Table II. There was no sign of cavitation damage.

The material compositions shown in Table III were normal. The results of the deposit analyses given in Table IV show that no sulfides or other unusual compounds were detected, but that the element sulfur was found in trace quantities. However, this sample did not have any of the other evidence usually associated with sulfide attack.

There was nothing unusual concerning the microstructures of the reducer or the pipe bend. There were narrow regions of grain growth at the welds. The hardnesses of the reducer and elbow away from their HAZ's were RB48-59 and RB37-48 respectively. These components were not in the fully annealed condition. There was a mild degree of softening in the HAZ's, with the reducer having a hardness of RB23 adjacent to the pipe bend weld, and the elbow having a hardness of RB33 on the other side of the weld. No distinct undercutting was present in the attacked region of the reducer. The pits were generally rounded and smooth, with light, rough corrosion attack occurring only in spots.

In summary, the damage to sample C2 is attributed to erosion-corrosion as a result of turbulence out of the SPS-49 cooler. A minor amount of under-deposit corrosion also occurred, but the metal removed due to this mechanism was insignificant compared to the erosion-corrosion damage. Stress-enhanced corrosion may also have been a factor in the attack of the reducer.

Sample C11. This 25" long sample is shown in Figure 8. It was horizontal on the ship. All of the joints were brazed. The joint fit-up at the flanges was good, but the coupling had up to a 3/16" gap as shown in Figure 8c. However, there was no significant attack downstream of the gap.

The only real damage to this sample began 2" back from the inlet flange, and affected the entire circumference of the pipe in a 2" wide band. Table III shows that the wall thickness was reduced to 0.017" in the deepest pit. The attacked area of the pipe had a brown/gold film, except for the pits themselves, which were black. The deposit downstream of the attacked area was a dull green/brown. The black deposit at the bottoms of the pits was fairly loose, and there were signs of recent active corrosion under it.

The compositions of the piping components of this sample were normal. No deposit analyses were performed on this sample. The hardness in attacked and non-attacked areas was RB47-59. The pipe had a normal microstructure throughout. A section taken through the pitted area showed that there was mild undercutting in the direction of flow. This section also showed that mild under-deposit corrosion had occurred.

The damage on this sample is attributed to erosion-corrosion caused by turbulence downstream of the orifice. Light under-deposit corrosion had also occurred, but this attack was insignificant compared to the erosion-corrosion.

Sample D1. The arrangement of sample D1 and views of the split halves are shown in Figure 9. The sample was positioned vertically on the ship. The braze joint fit-up at the inlet end was good. The braze joint at the elbow on the outlet end had a gap as great as 3/16", but there was no attack of the elbow downstream of the gap. The gap can be seen in Figure 9b. The boss weld did not penetrate to the ID.

The attack on this sample had an unusual distribution. As shown in Figures 9b and 9c, all of the damage was located in the middle portion of the pipe, with the material within 1.5" of either end being relatively unaffected. There was also a ring of relatively intact metal immediately opposite the boss weld, outside of which the most severe damage on the sample occurred. The pattern of the damage seems to suggest that the material in the HAZ's of the brazes and the weld was more resistant to whatever caused the attack than the non-heat-affected areas. The attacked areas had a dark brown/gold film with green spots, while the unaffected areas were lighter brown. Notes from the site at the time the pipe was first removed from the ship stated that the damaged area had a black color. There was very light corrosion under flakes of loose deposit. Some of these flakes had the typical crystalline maroon undersides, indicating redeposited copper. The damaged areas did not have the appearance of cavitation.

Table III shows that the compositions of the components of this sample were normal. No EDXA or X-ray analyses were performed on deposits from this sample.

The microstructure and hardness of the pipe was normal in both attacked and non-attacked areas. There was a large area of grain growth at the boss weld, but this was not one of severely damaged locations. A section taken through the ring of attack showed that the pits were slightly undercut in the direction of flow. Under-deposit corrosion was also observed. The damage was independent of grain boundaries.

The cause of the unusual distribution of attack is uncertain. Some turbulence was probably present in the flow coming out of the cooler; however, there appears to have been a definite protective effect in the

HAZ's. It is suggested that there may have been surface contamination of this piece of pipe prior to fabrication. Rather than baking onto the surface, this contaminant may have been volatilized or loosened due to the heat of brazing and welding. These areas may then have formed better protective films upon their first exposure to seawater than the non-heat affected areas.

Sample D5. Views of this sample are shown in Figure 10. The sample was over 9 feet long, and had been constructed in sections using 4 welds. The flanges were brazed on. This pipe had been positioned in the horizontal plane. All of the joints in the pipe were good.

There was one area of moderate attack on the bottom half of the pipe, affecting about 40% of the circumference immediately next to the inlet flange. The most severe attack began about 2" back from the inlet flange, and affected the entire circumference of the pipe similar to sample C11. Weld repair had been required in one location. Moderate damage and scattered pitting continued downstream of this area, tapering off within 5 inches. The attacked areas of the pipe were covered with a uniform black/brown film except for two spots in the bottom half of the pipe shown in Figure 10b. These spots had deeper attack with a scooped-out appearance, and had been worn down to bright gold metal. The nature of this damage suggests that the surrounding black film may have been cathodic to the bare metal, promoting galvanic corrosion of the metal in a spot where the black film had been removed. Closer examination of the pipe surface with a stereo-microscope revealed that the entire pipe within the black-film area was covered with small, distinct pits. The black film was loose in spots, and evidence of active corrosion was found beneath it.

Table III shows that the inlet flange and the first two pipe sections had normal compositions. Scrapings of the black film were analyzed by X-ray diffraction and EDXA. Nothing unusual was found by X-ray diffraction, but traces of sulfur were detected by EDXA. This information, combined with the fine distinct pits in the loose black film, suggests that sulfide-induced corrosion contributed to the attack.

The pipe had a normal microstructure both in and out of the braze HAZ. The baseline hardness was in the range RB38-62. The pits had a round and smooth profile and exhibited some directionality aligned with the flow. There was also microscopic evidence of rough general corrosion attack under the black deposit. This attack was independent of grain boundaries. A section taken through the gouged-out area in the pipe yielded similar results.

In summary, the major damage to this piece is attributed to erosion-corrosion due to turbulence downstream of the orifice. Sulfide corrosion is also thought to have played a role in causing the damage, along with under-deposit corrosion.

Sample G2. Figure 11 shows this sample, which had been positioned horizontally on the ship. This sample had three 90° elbows within a short distance of each other. There were seven brazed joints on this sample, all with good fit-up. The only joint with attack in its HAZ was at the outlet end of the sample just beyond the third elbow. As shown in Figure 11c, this attack was primarily located downstream of the intrados of the elbow. The area surrounding the attack had a uniform gold/brown film, but the attacked area had a loose black deposit in it.

The other area of attack on this sample occurred in the center of the short length of pipe between the first and second elbows. There were three pits on this area, all associated with a flaking dull brown deposit. The underside of this deposit had a crystalline, maroon appearance as already shown in Figure 26. Analysis of this deposit by EDXA showed that it was mainly copper. There was evidence of recent active corrosion under the loose deposit. No x-ray diffraction analyses of deposits were performed.

The compositions of the components of this sample were normal. The attacked pipe sections also had normal microstructures, and hardness levels of RB33-50. Metallographically, there were no signs of pit undercutting, but there was evidence of under-deposit corrosion in the middle pipe section.

In summary, the two areas of damage to this sample are attributed to two different sources. The pitting downstream of the third elbow is considered to be a result of turbulence downstream of the intrados of the elbow. In reference (a), this was demonstrated to be a typical site of turbulence. The pitting in the middle of the pipe between the two elbows is attributed to under-deposit corrosion.

Sample G4. This sample is shown in Figure 12. It was positioned horizontally on the ship. The flanges were brazed and had good joint fit-ups.

All of the damage to this sample occurred within 2.5' of the inlet end. The entire circumference was affected. The far end of the attacked area was out of the braze HAZ. The pipe was covered with a mottled green/brown/gold deposit which was fairly tight at the inlet end, and loose and flaking at the outlet end. This can be seen in Figures 11b and c. There was evidence of light corrosion under this deposit.

The compositions of the inlet flange and pipe were normal. X-ray diffraction of deposits collected from the pipe showed no unusual compounds. EDXA of the X-ray sample showed that trace quantities of sulfur were present. The outlet end of this sample was sent to NORDA for examination. No microorganisms were found colonizing the pipe. NORDA also performed EDXA of a small scraping of deposit from the pipe. As shown in Table IV, a significant quantity of manganese was detected in the specimen. NORDA rechecked these results, and determined that this was a localized condition which occurred in some spots; in other locations, no manganese at all was detected. The presence of manganese was always associated with the undersides of deposits. NORDA also noted that past studies on CuNi in seawater have shown that iron and manganese fixing bacteria can thrive under deposits and cause pitting. However, no bacteria or significant pitting were present on this sample in the area of the loose deposits.

Metallographic examination of sections through this sample showed that the pipe had a normal microstructure and that the pits at the inlet end were rounded and smooth. There was no undercutting.

The damage to this sample is attributed to erosion-corrosion caused by turbulence downstream of the orifice.

Sample J2. This 6 foot long sample is shown in Figure 13. The sample had been in a horizontal plane on the ship except for the outlet end, which turned downward. All of the joints on this sample were welded. The 90°

pipe elbow was a 2-piece construction made from stamped halves of sheet or plate material. The seam welds were double-butt welded, and they had been ground flush on the ID. This can be seen in Figure 13e. All of the joints exhibited good workmanship.

There were two areas of damage on this sample. The first and less severe involved shallow pitting near the inlet end of the pipe as shown in Figure 13c. This damage occurred beyond the HAZ of the flange weld, and affected most of the circumference of the pipe. The pitting gradually tapered off and stopped within 2 feet downstream of the inlet end. The surface of the pipe in this area had a speckled appearance as shown in Figures 13b and c; this film was fairly adherent, even in the pits.

The most severe damage on this sample occurred at the intrados of the outlet bend. The pipe had leaked at this location and had been repaired by ship's force. As shown in Figures 13e and 13f, this attack had the appearance of small, closely-grouped round pits. The figures also show that the seam weld in the bend and the HAZ of the pipe opposite the flange weld were less severely pitted. This is more clearly illustrated in Figure 28, which shows a cross-section of the outlet pipe flange weld. This was not a full penetration weld. The pitted area did not have a significant build-up of deposit, but the area surrounding it had a flaking dull green/brown deposit.

Table III shows that the EDXA chemistries of the components were normal. Scrapings of deposits from both ends of the pipe were collected and analyzed separately. As shown in Table IV, there were no unusual results obtained by NAVSSES. However, one half of the lightly pitted inlet end of the sample had been sent to NORDA for examination, where a trace of sulfur was found in a surface EDXA of the deposits. This sulfur is not considered to have caused any of the pitting. NORDA also found that rod-shaped bacteria were colonizing the surface of the pipe, but could not determine whether the organisms had contributed to the damage. Figure 29 depicts the organisms detected by NORDA.

The straight inlet portion of the pipe had a normal microstructure with a hardness of RB23-43. The shallow pitting in this part of the pipe was independent of grain boundaries and was out of any weld HAZ's. There was some evidence of under-deposit corrosion in the shallow pits. The outlet bend of this sample had a baseline hardness of RB60-69. The high hardness level is a result of cold work used to form the piece, and shows that the fitting was not installed in the fully annealed condition as required by reference (e). The HAZ's of the welds in the bend had hardnesses of RB23-43. The softening is due to partial annealing of the metal by the heat of welding. The pipe bend had a normal microstructure throughout, even in the HAZ's. Cross-sections of the pits at the outlet showed that they were smooth and round. An example is shown in Figure 30.

It was already noted that the pipe metal in the weld HAZ's was less attacked than the surrounding metal. When sections through the welds were etched for metallographic examination, the HAZ's etched much lighter than the adjacent metal. This indicates that the HAZ metal was noble to the surrounding area, and less prone to corrosion. This is a common occurrence when metal with significant residual stress is welded. Highly stressed areas are more prone to corrosion than non-stressed areas within the same piece of metal, which causes the mechanism known as stress-enhanced corrosion. This accounts for the uneven distribution of the attack around the HAZ. The fact

that this pitting was limited to the intrados of the elbow on the end where the flange was welded may be related to additional residual stresses introduced as a result of weld shrinkage. The pipe bend had a large radius, and therefore should not have caused turbulence. In addition, there were no nearby turbulence promoters upstream, and there was no evidence to support sulfide attack.

Check Valves. The check valves were from the forward and aft AEGIS piping systems, but were not specifically identified as to which of the two systems each came from. They were the first check valves downstream of the AEGIS pumps, and were reported to have been in service for 6 to 8 months. The internal components of the valves had come loose, and the various pieces were found elsewhere in the piping system or in the compartments in which the valves were located. The name "DeSanno" was cast into the valves.

Examination of the valve bodies showed that there had been significant wear of the sides of the valves where the flappers are held in place by the pins. There were corresponding wear marks on the flapper hinges and the single pin recovered. The components were re-installed in the laboratory, and it was found that the pin could be made to come loose with very little play. This was a direct result of the wear of the mating parts.

The hinge pin was 2.61 inches long and 0.375 inches in diameter. EDXA showed that the pin was Monel, and that the flapper hinges and valve bodies were bronze casting alloys. The valve bodies had very little allowance for wear caused by the hinge and hinge pin, and therefore "failed" prematurely. It is recommended that longer hinge pins be used, along with valve bodies which have larger cavities to accommodate them.

#### DISCUSSION AND SUMMARY

Review of Table III shows that erosion-corrosion caused by turbulence was considered to be the primary source of damage to the piping. This type of attack was usually located within a foot downstream of a turbulence causing component. Orifices, butterfly valves and 90° degree elbow flex hose fittings were all identified as turbulence promoters. The forward AEGIS pump caused impingement damage, a related mechanism.

The attacked pipes were in systems which represented flow rates of 6 fps to 10.4 fps. While these flow rates are within the 15 fps limit set by reference (d), the localized flow rates caused by turbulence are probably far higher. As noted in the Background section of this report, and as discussed in reference (a), it is generally agreed that the 15 fps design limit is too high for pipe sizes under six inches. A revision of reference (d) should be undertaken as soon as acceptable velocity limits are agreed upon, as this document will affect all new ship construction. Three potential solutions to the present problem are offered.

a) Use of component designs which cause less turbulence. Low turbulence orifices in particular are available, as was discussed in reference (a).

b) Use of a compatible, more erosion resistant material for the piping located 1 to 2 feet immediately downstream of the problem components. 70-30 CuNi is recommended on a trial basis.

c) Use of nylon or other polymeric inserts in the inlet ends of piping downstream of problem components. This approach has been tried with some success on the inlet ends of tubes in air conditioning heat exchangers.



MIC and sulfide induced corrosion were both implicated in this analysis, but were not proven. Although colonies of bacteria were found on some samples, they were not shown to have caused corrosion. However, the limited number of dried-out, months-old samples used in the MIC study were not ideal for producing conclusive results. NORDA will be doing additional work on this topic with specimens freshly obtained from the PSA on USS VALLEY FORGE (CG-50) in September 1986. This study should help decide whether MIC is, in fact, a factor that needs to be dealt with in solving this problem. Regarding sulfide induced corrosion, extensive deposit analyses have been performed on piping from CG-48 and CG-49. Both X-ray diffraction for compounds and EDXA for elements were used, but sulfide compounds were never detected. The main evidence used to implicate sulfide corrosion has been the presence of the element sulfur in trace quantities, in combination with loose black films or well-defined, sharp-edged pits. Therefore, it is recommended that deposit analyses be kept to a minimum until more accurate laboratory methods are available.

In reference (b), attack of metal in the HAZ's of welds and brazes was considered to be circumstantial, and was thought to be more a result of the necessity of having a joint at the inlet end of a run of pipe. Therefore, a turbulence-causing component upstream of the damaged area would be responsible for the attack rather than the HAZ itself. This premise was supported in this analysis. Table IV gives the condition of all the weld and braze joints which were present in CG-49 PSA samples. There were more non-attacked than attacked joints, and most of the damaged joints involved the inlet ends of the samples. One should also keep in mind that only deteriorated piping was sent to NAVSSES as a result of the PSA, and that far more welded and brazed joints were contained in intact piping left on the ship.

Stress-enhanced corrosion is a new issue which has been raised in this investigation. As noted earlier, reference (e) requires that 90-10 CuNi reducers, elbows and other fittings be furnished in the fully annealed condition. Material in this condition should have hardness levels of RB15-25. However, the reducer samples (A2, B3, C2) from the CG-49 had baseline hardnesses ranging from RB48 to RB74, and the elbow of sample J2 had a baseline hardness of RB60-69. These components were probably installed by Ingalls, and were obviously not in the fully annealed condition. The hardness levels indicate that the pieces were in the lightly drawn condition. The increased hardnesses are the result of residual stresses in the metal from cold-working operations such as swaging, stamping and bending. The HAZ's of brazes and welds in these fittings were softer, the result of partial annealing of the metal in these local areas.

Metal which contains residual stresses will be more prone to corrosion than metal which does not. This results in stress-enhanced corrosion. The pitting of the outlet end of sample J2 was not caused by any upstream component. In addition, although the damage to samples A2, B3 and C2 was partly attributed to turbulence, the components responsible were located at least 5 inches upstream, further in the case of A2. It is considered that stress-enhanced corrosion was also a factor in these samples. As shown in Figure 1d for sample A2, and Figures 13e and 28 for sample J2, the partly annealed HAZ's of these samples were less severely attacked than the metal outside of the HAZ's. It is recommended that fully annealed fittings be installed in the future, and that the performance of these fittings be monitored.

## REFERENCES

- (a) Proceedings of the AEGIS Cruiser Seawater Corrosion Workshop, NAVSEA PMS-400C, Sponsor, 27-29 May 86
- (b) "Investigation of Seawater Piping Deterioration on USS YORKTOWN (CG-48) and USS VINCENNES (CG-49)", NAVSSES memo 10310, 053B/Ser 3092 of 26 Mar 86
- (c) NAVSSES AEGIS Information Form 86-005 of 6 Feb 86
- (d) General Specification for Ships of the United States Navy, Section 505b3, NAVSEA 0910-LP-007-4100, Mar 84
- (e) Navy Standard Drawing 810-1385880, Rev. D, "Fittings, Copper-Nickel Alloy, Slip-On Sleeve for Brazing, Arc or Gas Welding, 200 PSI at 150°."
- (f) NORDA ltr 3910, Ser 333/476 of 4 Jun 86

## BIBLIOGRAPHY

Proceedings of the AEGIS Cruiser Seawater Corrosion Workshop, NAVSEA PMS-400C, Sponsor, 27-29 May 86

M. R. Brown, Jr., Masters Degree Thesis, Massachusetts Inst. Tech., "Investigation of the Accelerated Corrosion of Cupro-Nickel Piping", DTIC Report AD-A097300, Jun 79

J. A. Ellor, G. A. Gehring, Jr., and B. C. Syrett; "An Investigation of Water Treatments for Mitigating Sulfide-Related Corrosion of Copper Alloy Condenser Tubes"; Paper presented at "Corrosion/86" Corrosion Conference sponsored by NACE

M. G. Fontana and N. D. Greene, "Corrosion Engineering", 2nd Ed., McGraw-Hill Book Co., NY, NY 78

S. Gerchakov, B. Little, P. Wagner, "Probing Microbiologically Induced Corrosion", Unpublished Paper

Gibbs and Cox, Inc., Conference Report; FFG7/256, 521 (4-JBD-3195), 19723-734 of 30 May 85 (Surface Ship Seawater System Deterioration (4SD) Program Steering Committee Meeting). Contains "Corrosion and Corrosion Prevention for CG-47 Class Cruisers: A Preliminary Assessment", R. M. Kain, LaQue Center for Corrosion Technology, Inc. for Ingalls Shipbuilding, May 85

Gibbs and Cox, Inc., Trip Report; FFG7/256-521 (4-JBD-3220), 19723-734 of 14 Jun 85 (Inspection of Seawater Piping Removed from CG-48)

H. Hack, "Effectiveness of Ferrous Sulfate as an Inhibitor for Sulfide-Induced Corrosion of Copper-Nickel Alloys", DTNSRDC Report 77-0072 of Jul 77

H. Hack and J. Gudas, "Inhibition of Sulfide-Induced Corrosion of Copper-Nickel Alloys with Ferrous Sulfate", Materials Performance, Pg. 25-28, Mar 79

H. Hack and J. Gudas, "Inhibition of Sulfide-Induced Corrosion by Clean Seawater Pre-Exposure", DTNSRDC Report SME-79-85 of Nov 79

H. Hack, "Galvanic Corrosion of Piping and Fitting Alloys in Sulfide-Modified Seawater", J. Testing and Eval., Vol 8, No.2, Pg 72-79, Mar 80

H. Hack and J. Gudas, "Inhibition of Sulfide-Induced Corrosion with a Stimulated Iron Anode", Materials Performance, Vol 19, No.4, Pg 49-54, Apr 80

H. Hack and T. S. Lee, "Effect of Ferrous Sulfate on Sulfide-Induced Corrosion of Copper-Base Condenser Alloys in Aerated Seawater", DTNSRDC Report SME-81/91 of Jan 82

H. Hack, "The Effect of Brief Discontinuation of Ferrous Ion Application on Sulfide-Induced Corrosion of Copper-Nickels", DTNSRDC Report SME-81/120, Mar 82

V. Karakelian, "Investigations Into Heat Exchanger and Piping Failures on USS YORKTOWN (CG-48)", NAVSSES Final Report of Mar 85

"Accelerated Corrosion of Copper-Nickel Piping", National Materials Advisory Board Report NMAB-343, Dec 77

"Investigation of Seawater Piping Deterioration on USS YORKTOWN (CG-48) and USS VINCENNES (CG-49)", NAVSSES memo 10310, 053B/Ser 3092 of Mar 86

D. Pope, "Microbiologically Induced Corrosion: Detection, Treatment and Prevention", Unpublished Paper

Surface Ship Sea Connected Piping System Deterioration Investigation, Annual Report for FY 82, NAVSEA 56YD, Sep 82

Surface Ship Sea Connected Piping System Deterioration Investigation, Interim Report for FY 83, NAVSEA 56YD, Apr 83

B. Syrett, "The Mechanism of Accelerated Corrosion of Copper-Nickel Alloys in Sulfide-Polluted Seawater", Paper No.33 Presented at "Corrosion/80" Mar 3-7, 80

USS TICONDERGOA msg 041733Z Dec 85, Subj: Salt Water Cooling Piping Leaks

D. C. Vreeland and Cdr. E. Ogden, "Seawater Corrosion of 90/10 Copper-Nickel Piping - A Survey", DTNSRDC Ltr Report TM-28-74-307

D. Vreeland, "Review of Corrosion Experience with Copper-Nickel Alloys in Seawater Piping Systems", Materials Performance, Pg. 38-41, Oct 76

TABLE I: CG-49 PSA PIPING SPECIMENS

<u>ID</u>	<u>System and Location</u>
A2	Fwd. AEGIS, Inlet pipe to cooler.
A4	Fwd. AEGIS, Pipe downstream of cooler discharge dogleg.
A14	Fwd. AEGIS, Pipe downstream of AEGIS pump.
A16	Fwd. AEGIS, Fwd. AEGIS pump room, pipe downstream of butterfly valve and upstream of strainer.
B3	Aft AEGIS, Outlet pipe from cooler.
B4	Aft AEGIS, Pipe downstream of cooler discharge dogleg.
B5	Aft AEGIS, Pipe downstream of cooler discharge butterfly valve.
B19	Aft AEGIS, Pipe downstream of the orifice downstream of cooler.
C2	SPS-49, Outlet pipe from cooler.
C11	SPS-49, Pipe downstream of 1st orifice downstream of cooler.
D1	SQS-53, Outlet pipe from cooler.
D5	SQS-53, Pipe downstream of 2nd orifice upstream of cooler.
G2	HPAC #2, Outlet pipe from cooler.
G4	HPAC #2, Pipe between two discharge orifices.
J2	A/C, Pipe downstream of 1st discharge orifice.
-	Fwd. AEGIS, 3-inch check valve (Un-marked)
-	Aft AEGIS, 3-inch check valve (Un-marked)

TABLE II: COPPER-NICKEL CORROSION PRODUCT FILMS AND ANALYSES

<u>Description</u>	<u>Analysis</u>	<u>Source</u>
Tan-brown or Sandy	$\text{Cu}_2\text{O}$	Cuprous oxide. Normal film formed by 90-10 CuNi.
Orange-brown or Reddish-brown	$\text{FeO}\cdot\text{OH}$	Lepidocrocite. Film deposited by ferrous sulfate injection.
Loose black film	$\text{Cu}_2\text{O} + \text{S}^*$	Sulfur-bearing film formed in seawater contaminated by sulfide.
Maroon or Purple	Cu, Cu-Ni	Redeposited copper or CuNi grains. Usually found on underside of deposits.
Green-Blue	$\text{Cu}_2(\text{OH})_3\text{Cl}$	Copper Hydroxychloride. Minor corrosion product of copper in seawater.
Yellow-Brown	$\text{CuCl}_2$	Cupric chloride. Minor corrosion product of copper in seawater.
Green-Blue	$\text{CuCl}_2\cdot 2\text{H}_2\text{O}$	Cupric chloride dihydrate. Minor corrosion product of copper in seawater.
Gray-Black	$\text{CuO}$	Cupric oxide. High temperature oxide of copper.

\* No compound identified, but sulfur reported as present via EDXA.  
One author estimated 0.28% sulfur.

TABLE III - SAMPLE BACKGROUND, COMPOSITION, WALL THICKNESSES & SUMMARY

Sample ID	Min. Spec. Flow Rate (fps)	Component	Chemistry	Minimum/Nominal Wall Thk (in.)*	Min. Measured Wall Thk. (in.)	SUMMARY Cause of Deterioration
A2	10.4 (in. Pipe)	3" Pipe	90-10 (1.4% Fe)	0.095	0	Erosion-corrosion of pipe caused by turbulence. Under-deposit and sulfide corrosion also on pipe and reducer. Stress-enhanced pitting of reducer possible.
		4"x3" Reducer Inlet Flange	90-10 (1.3% Fe) Tin Bronze	0.125	0.105	
		Outlet Flange	90-10 (1.3% Fe)	-	-	
A4	10.4	3" Pipe	90-10 (1.7% Fe)	0.095	0	Erosion-corrosion due to turbulence from upstream flex hose elbow.
		Inlet Flange Outlet Flange	Tin Bronze Tin Bronze	- -	- -	
A14	10.4 in 3" 16.7 in 2.5"	2.5"x3" Reducer	90-10 (1.1% Fe)	0.098	0	Erosion-corrosion due to impingement, and cavitation downstream of pump.
		3" Nipple	90-10 (1.6% Fe)	0.095	0.098	
		Inlet Flange	90-10 (1.8% Fe)	-	-	
A16	10.4	3" Pipe w/Bend	90-10 (1.1% Fe)	0.095	0	Erosion-corrosion due to impingement downstream of butterfly valve.
		Inlet Flange	90-10 (1.0% Fe)	-	-	
B3	10.4 (in Pipe)	4"x3" Reducer	90-10 (1.4% Fe)	0.142	0.028	Reducer: Sulfide and turbulence induced erosion-corrosion. Possible stress-enhanced corrosion. Pipe: Sulfide and high flow rate induced erosion-corrosion.
		3" Pipe	90-10 (1.6% Fe)	0.095	0.070	
		Inlet Flange Outlet Flange	90-10 (1.5% Fe) Tin Bronze	- -	- -	
B4.1	10.4	3" Pipe	90-10 (1.3% Fe)	0.095	0	Local turbulence due to flow meter parts trapped at outlet end.
		Inlet Flange Outlet Flange	Tin Bronze Tin Bronze	- -	- -	
B4.2	10.4	3" Pipe Inlet Flange Outlet Flange	90-10 (1.3% Fe) Tin Bronze Tin Bronze	0.095 - -	0 - -	Uncertain. Under-deposit corrosion, turbulence and sulfide implicated. Initial film formation suspect.

TABLE III - SAMPLE BACKGROUND, COMPOSITION, WALL THICKNESSES & SUMMARY

Sample ID	Min. Spec. Flow Rate (fps)	Component	Chemistry	Minimum/Nominal Wall Thk (in.)*	Min. Measured Wall Thk. (in.)	SUMMARY Cause of Deterioration
B5	10.4	3" Pipe w/Bend Inlet Flange	90-10 (1.5% Fe) 90-10 (1.6% Fe)	0.095 -	0 -	Erosion-corrosion due to impingement downstream of butterfly valve.
B19	10.4	3" Pipe Inlet Flange	90-10 (1.1% Fe) Tin Bronze	0.095 -	0 -	Erosion-corrosion due to turbulence downstream of orifice. Isolated pits caused by sulfide corrosion.
C2	8.9	3"x2" Reducer 2" Pipe w/Bend Inlet Flange	90-10 (1.2% Fe) 90-10 (1.4% Fe) 90-10 (1.5% Fe)	0.130 0.011 - 0.135 -	0.080 0.110(outer bend) -	Erosion-corrosion due to turbulence out of cooler. Minor under-deposit corrosion. Possible stress-enhanced corrosion of reducer.
C11	8.9	2" Pipe Inlet Flange	90-10 (1.5% Fe) Tin Bronze	0.083 -	0.017 -	Erosion-corrosion due to turbulence downstream of orifice.
D1	8.9	2.5" Pipe Inlet Flange	90-10 (1.2% Fe) Tin Bronze	0.083 -	0.029 -	Uncertain: Turbulence downstream of cooler a factor. Initial film formation suspect.
D5	8.9	2.5" Pipe (1st) 2.5" Pipe (2nd) Inlet Flange	90-10 (1.4% Fe) 90-10 (1.4% Fe) Tin Bronze	0.083 0.083 -	0 Not Performed -	Erosion-corrosion due to turbulence downstream of orifice. Sulfide and under-deposit corrosion also acting.
G2	6.0	Inlet Flange 1.5" Nipple #1 Elbow #1 1.5" Pipe Elbow #2	Tin Bronze 90-10 (1.0% Fe) Tin Bronze 90-10 (1.2% Fe) Tin Bronze	- 0.072 - 0.072 -	- Not Performed - 0.039 -	Erosion-corrosion due to turbulence downstream of elbow intrados in 1' spot; under-deposit corrosion in other location.



TABLE III - SAMPLE BACKGROUND, COMPOSITION, WALL THICKNESSES & SUMMARY

Sample ID	Min. Spec. Flow Rate (fps)	Component	EDXA Chemistry	Minimum/Nominal Wall Thk (in.)*	Min. Measured Wall Thk. (in.)	SUMMARY Cause of Deterioration
G4	6.0	1.5" Pipe Inlet Flange	90-10 (1.1% Fe) Tin Bronze	0.072	0.014	Erosion-corrosion due to turbulence downstream of orifice.
J2	6.1	6" Pipe(Inlet) 6" Pipe Bend (Outlet) Inlet Flange Outlet Flange	90-10 (1.4% Fe) 90-10 (1.6% Fe) 90-10 (1.7% Fe) 90-10 (1.7% Fe)	0.134 0.122 (Side of Bend) - -	0.112 0 - -	Inlet pitting: Uncertain. MIC and/or under-deposit corrosion suspect. Outlet: Stress-enhanced corrosion.

\* = The minimum/nominal wall thickness reported for reducers and pipes with bends is the minimum measured thickness.

For straight pipes, this value is the minimum specification limit.

TABLE IV: CHEMICAL ANALYSES OF DEPOSITS

<u>Sample ID</u>	<u>EDXA of Deposits (Elements)</u>	<u>X-Ray Diffraction (Crystalline Compounds)</u>
A2	<u>Reducer-Powdered X-ray Sample</u>	
	Major: Cu, Fe	Cu <sub>2</sub> O
	Minor: Ni, Cl	Cu <sub>2</sub> (OH) <sub>3</sub> Cl
	Trace: Si, Ca	
	<u>Pipe-Powdered X-ray Sample</u>	
	Major: Cu, Fe	Cu <sub>2</sub> O
	Minor: Ni, Cl	
	Trace: Si, Ca	
	<u>Surface of Black Deposit</u>	
	Major: Cu, Fe	Not Performed
	Minor: Ni, Cl	
	Trace: Si, S, Ca	
A4	<u>Underside of Black Deposit</u>	
	Major: Cu, Fe	Not Performed
	Minor: Ni, Cl	
	Trace: S, Ca, Si	
	<u>Inlet side of Pipe- top half Powdered X-ray Sample</u>	
	Major: Cu, Ni, Fe	Cu <sub>2</sub> O
	Minor: Cl	Cu
	Trace: Si, S, Ag, Ca, Mn	Cu <sub>2</sub> (OH) <sub>3</sub> Cl
	<u>NORDA Analysis of Deposit Surface</u>	
	Major: Cu, Ni, Fe	Not Performed
	Minor: P	
	Trace: Al, Si, S, Cl, K, Ca	
A14	<u>Deposit from Reducer and Nipple</u>	
Major: Cu	Not Performed	
Minor: Fe, Ni, Cl		
Trace: Si, Ca		
B3	<u>Pipe-Powdered X-ray Sample</u>	
	Major: Cu, Fe	Cu <sub>2</sub> O
	Minor: Ni, Cl	Cu <sub>2</sub> (OH) <sub>3</sub> Cl
	Trace: Si, Ag, Ca	Cu
	<u>Reducer-Powdered X-ray Sample</u>	
	Major: Cu, Fe, Ni	Cu <sub>2</sub> O
Minor: Cl	Cu	
Trace: Si, Ca, Mn		

<u>Sample ID</u>	<u>EDXA of Deposits (Elements)</u>	<u>X-Ray Diffraction (Crystalline Compounds)</u>
B3	<u>Surface of Black Deposit on Pipe</u> Major: Fe, Cu Minor: Ni, Cl Trace: Al, Si, S, K, Ca	Not Performed
	<u>Surface of Orange/Brown Deposit on Pipe</u> Major: Fe, Cu Minor: Si Trace: Al, S, K, Ca, Ni, Cl	Not Performed
B4.2	<u>Powdered X-ray Sample</u> Major: Cu Minor: Fe, Cl Trace: Si, Sn, Ca	Cu <sub>2</sub> O Cu <sub>2</sub> (OH) <sub>3</sub> Cl
	<u>Maroon Underside of Deposit Flake</u> Major: Cu Minor: Fe Trace: Ni, Cl	Not Performed
	<u>White Splotches on Pipe</u> Major: Ti Minor: Fe, Cu Trace: -	Not Performed
	<u>Deposit at Outlet Flange</u> Major: Cu, Fe, Cl Minor: Al, Si, Ca, Ni Trace: S, K	Not Performed
	<u>Pipe at Inlet end-X-ray Sample</u> Major: Cu, Fe, Ni Minor: Cl Trace: Si, S, Ca	Cu <sub>2</sub> O Cu-Ni
C2	<u>Reducer and Bend-X-ray Sample</u> Major: Cu, Fe, Ni Minor: Si, Cl Trace: S, Ca, Ti, Zn	Cu <sub>2</sub> (OH) <sub>3</sub> Cl Cu <sub>2</sub> O
D5	<u>Inlet Pipe-Powdered X-ray Sample</u> Major: Cu, Fe, Ni Minor: Cl Trace: Si, Mn, S	Cu Cu <sub>2</sub> (OH) <sub>3</sub> Cl Cu <sub>2</sub> O
G2	<u>Spherical particles in Maroon Underside of Deposit Flake</u> Major: Cu Minor: - Trace: Fe	Not Performed

<u>Sample ID</u>	<u>EDXA of Deposits (Elements)</u>	<u>X-Ray Diffraction (Crystalline Compounds)</u>
G4	<u>Powdered X-ray Sample</u> Major: Cu Minor: Cl, Fe, Ni Trace: Si, S, Ag, Zn	Not Performed
	<u>NORDA-Small Area of Deposit Scrapings</u> Major: Cu, Fe, Mn Minor: Ni Trace: K, Ca	Not Performed
J2.1	<u>Inlet end of Pipe-X-ray Sample</u> Major: Cu Minor: Fe, Ni Trace: Si, Cl	Cu <sub>2</sub> O Cu <sub>2</sub> (OH) <sub>3</sub> Cl Cu
	<u>NORDA Analysis of Deposit Surface</u> Major: Cu, Fe, Cl, Ni Minor: Ca, Si Trace: Al, P, S, K	Not Performed
J2.4	<u>Outlet end of Pipe-X-ray Sample</u> Major: Cu Minor: Cl, Fe, Ni Trace: Si, Ca	Cu <sub>2</sub> O Cu <sub>2</sub> (OH) <sub>3</sub> Cl Cu

**TABLE V: CONDITION OF WELDED AND BRAZED JOINTS**

<u>Welded - Attacked</u>		<u>Welded - Intact</u>	
<u>ID</u>	<u>Description</u>	<u>ID</u>	<u>Description</u>
A14	Inlet, cavitation one side	A2	Mid-sample
A16	Inlet, partial damage	A2	Outlet
B3	Inlet, partial damage	A14	Mid-sample
B3	Mid-sample joint	A14	Outlet
B5	Inlet, partial damage	B5	Mid-sample (2 welds)
C2	Inlet	B5	Outlet
C2	Mid-sample, reducer side	B19	Mid-sample (2 welds)
D1	Mid-sample, boss	C2	Mid-sample, 45° pipe elbow
J2	Outlet intrados, flange and seam	D5	Mid-sample, boss
		D5	Mid-sample (3 welds)
		J2	Inlet
		J2	Mid-sample
		J2	Outlet extrados, seam weld
 <u>Brazed - Attacked</u>		 <u>Brazed - Intact</u>	
A2	Inlet	A4	Outlet
A4	Inlet	C11	Inlet
B3	Outlet	C11	Mid-sample (2 brazes-coupling)
B4.1	Inlet	C11	Outlet
B4.1	Outlet	D5	Outlet
B4.2	Inlet	G2	Inlet
B4.2	Outlet	G2	Mid-sample (5 brazes at elbows)
B19	Inlet, partial damage	G4	Outlet
D5	Inlet, partial damage		
G2	Outlet		
G4	Inlet		

CG-49 PSA  
SEAWATER PIPING ANALYSIS  
X-RAY DIFFRACTION RESULTS

Attachment (A)

5200  
053D/Ser 3214  
20 JUN 1986

MEMORANDUM

From: 053D (M. Holtsberg)  
To: [REDACTED]

Subj: X-RAY DIFFRACTION ANALYSES OF WATERSIDE DEPOSITS FROM CG-49 Cu-Ni  
SEAWATER PIPING

Ref: (a) Service request from N. Clayton (053B) of 14 May 86

Encl: (1) One through Twelve: X-ray powder diffractograms of unknown  
samples with powder diffraction standards

1. X-ray diffraction analyses were performed on 12 (twelve) CG-49 Seawater piping waterside deposits, in compliance with reference (a). Reference (a) requested a search for sulfides, sulfates and ammonia compounds. None of these were found. The crystalline compounds found were as follows:

<u>053B Identification</u>	<u>053D XRD Designation</u>	<u>Compounds found</u>
A2 Inlet Reducer - Loose Deposits	SM-514A	Cu <sub>2</sub> O, Cu <sub>2</sub> (OH) <sub>3</sub> Cl
A2 Outlet Pipe - Loose Deposit	SM-515B	Cu <sub>2</sub> O
A4 Top Half Inlet Pipe	SM-519C	Cu <sub>2</sub> O, Cu, Cu <sub>2</sub> (OH) <sub>3</sub> Cl
B3 Outlet Pipe - Loose Deposit	SM-520A	Cu <sub>2</sub> O, Cu <sub>2</sub> (OH) <sub>3</sub> Cl, Cu
B3 Inlet Reducer	SM-520B	Cu <sub>2</sub> O, Cu
B4.2 Top Half - Loose Deposit	SM-521A	Cu <sub>2</sub> O, Cu <sub>2</sub> (OH) <sub>3</sub> Cl
B19.1 Bottom Pipe	SM-522A	Cu <sub>2</sub> O, Cu-Ni
C2 Elbow and Reducer	SM-522B	Cu <sub>2</sub> (OH) <sub>3</sub> Cl, Cu <sub>2</sub> O
G4 Bottom Loose Deposit	SM-523A	Cu <sub>2</sub> O, Cu <sub>2</sub> (OH) <sub>3</sub> Cl
J2.1 Pipe Top	SM-527A	Cu <sub>2</sub> O, Cu <sub>2</sub> (OH) <sub>3</sub> Cl, Cu
J24	SM-528A	Cu <sub>2</sub> O, Cu <sub>2</sub> (OH) <sub>3</sub> Cl, Cu
D5.1 Top and Bottom Pipe Halves	SM-528B	Cu, Cu <sub>2</sub> (OH) <sub>3</sub> Cl, Cu <sub>2</sub> O

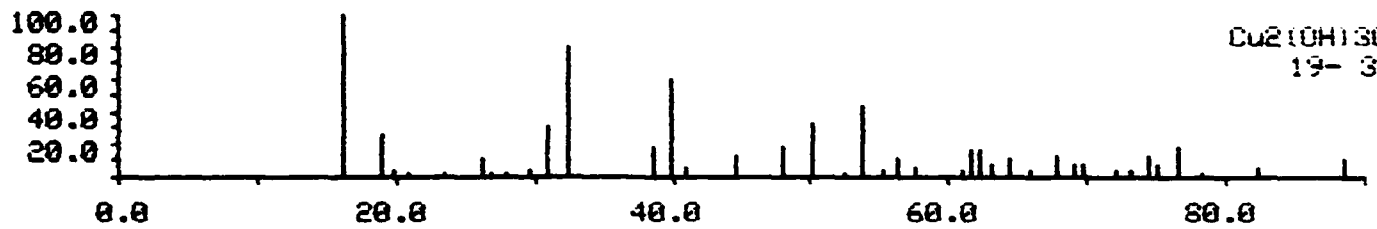
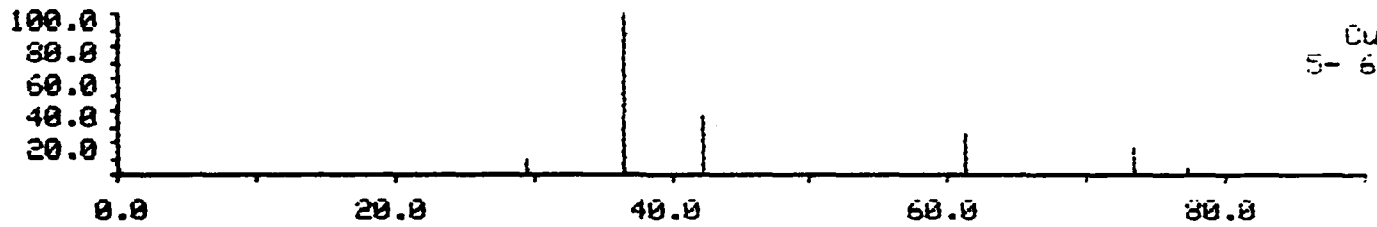
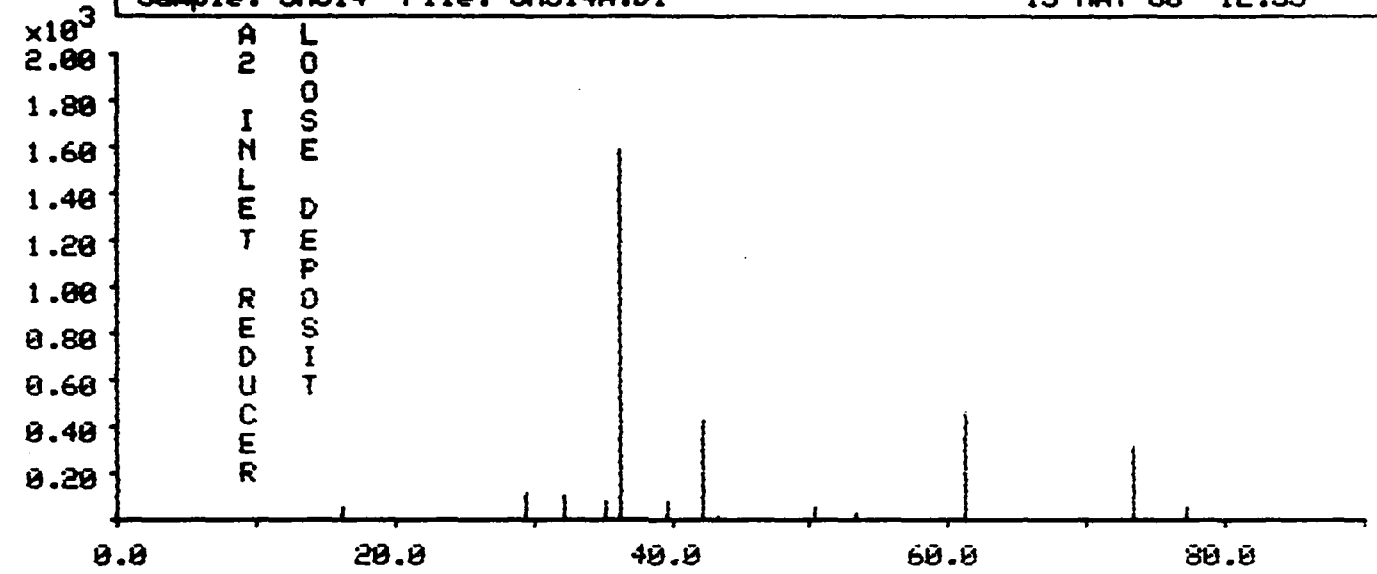
*M. Holtsberg*  
M. HOLTSBERG

Copy to:  
053, 053D(2)

①

Sample: SM514 File: SM514A.DI

15-MAY-86 12:55

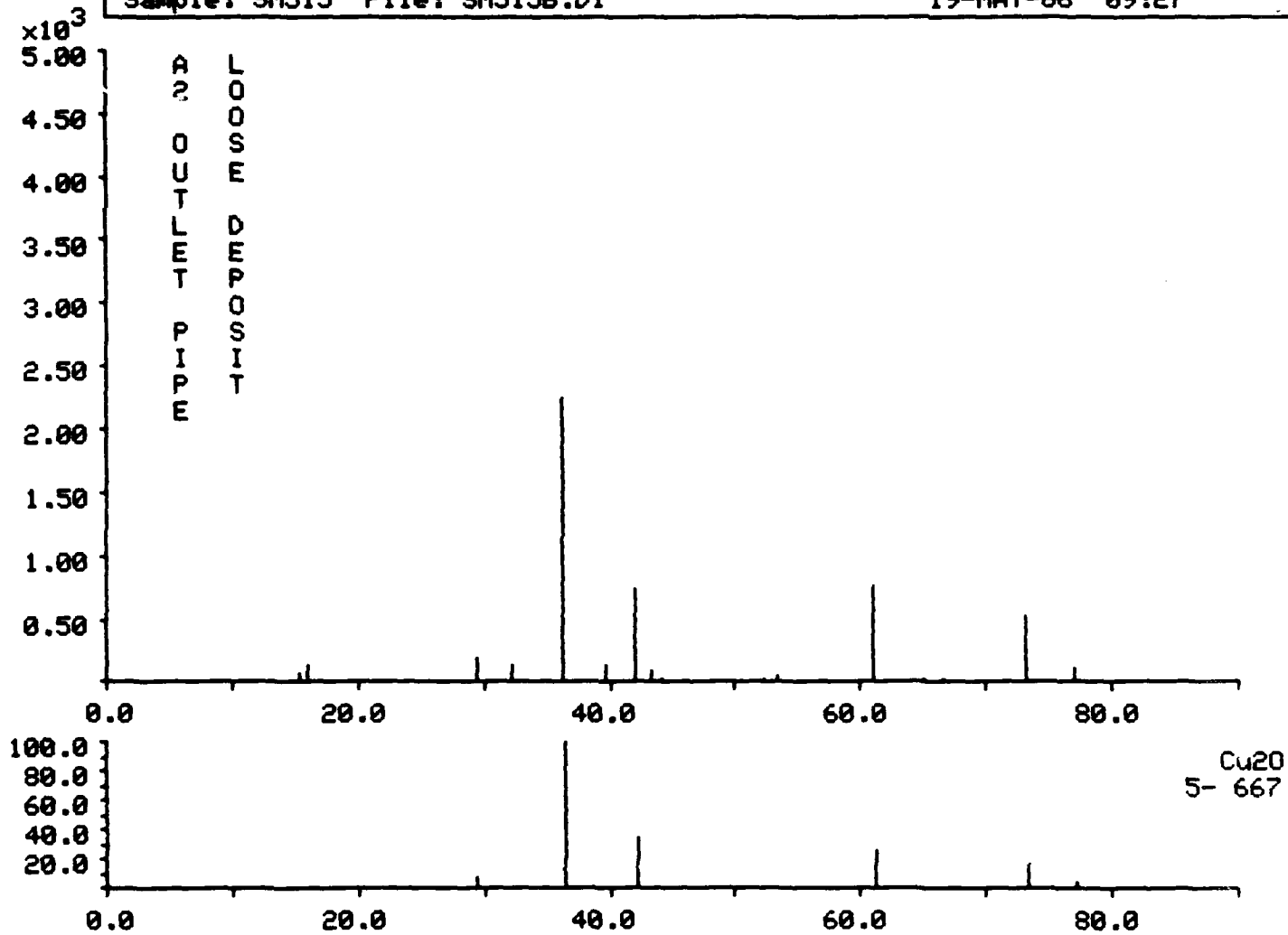


Encl(1)



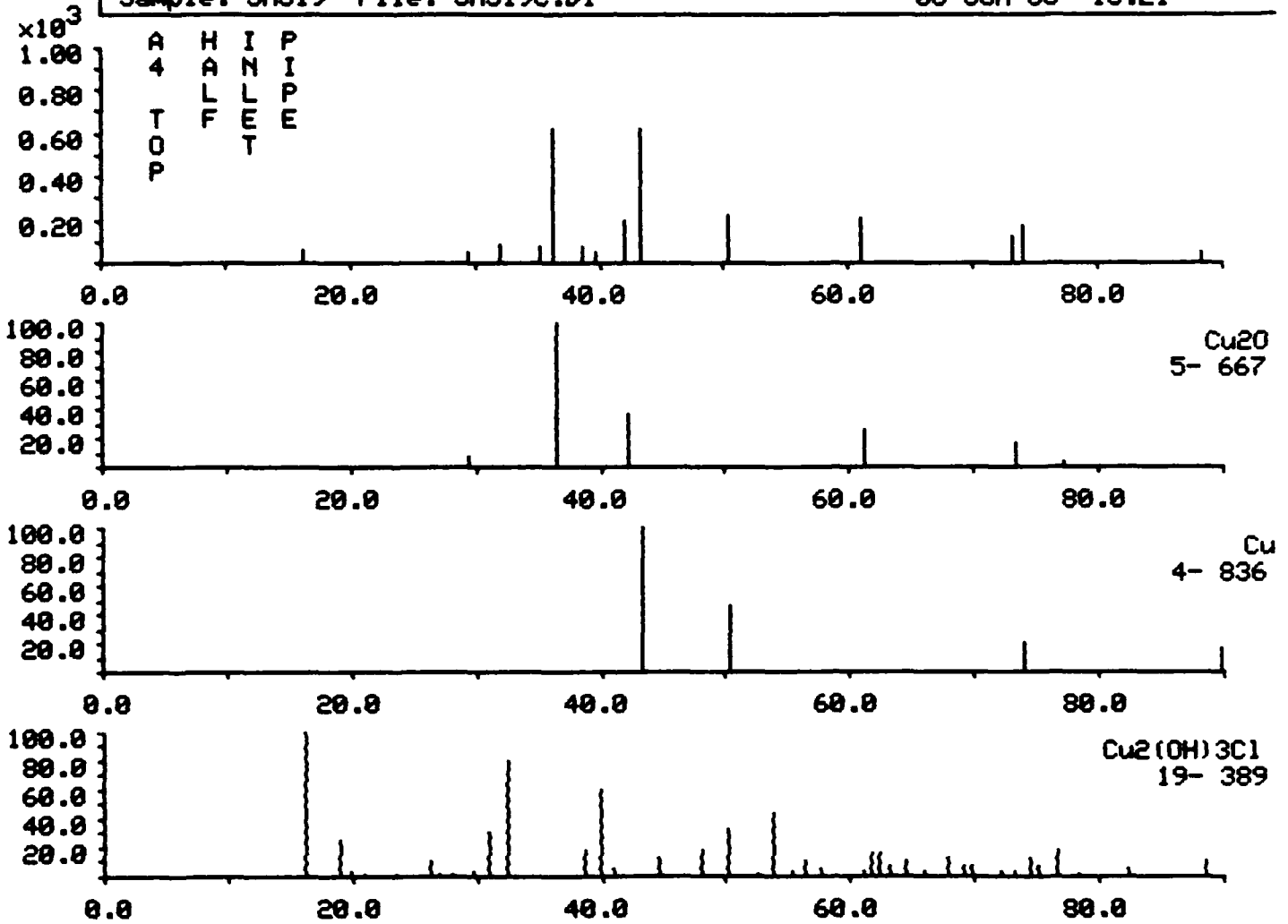
Sample: SM515 File: SM515B.D1

19-MAY-86 09:27



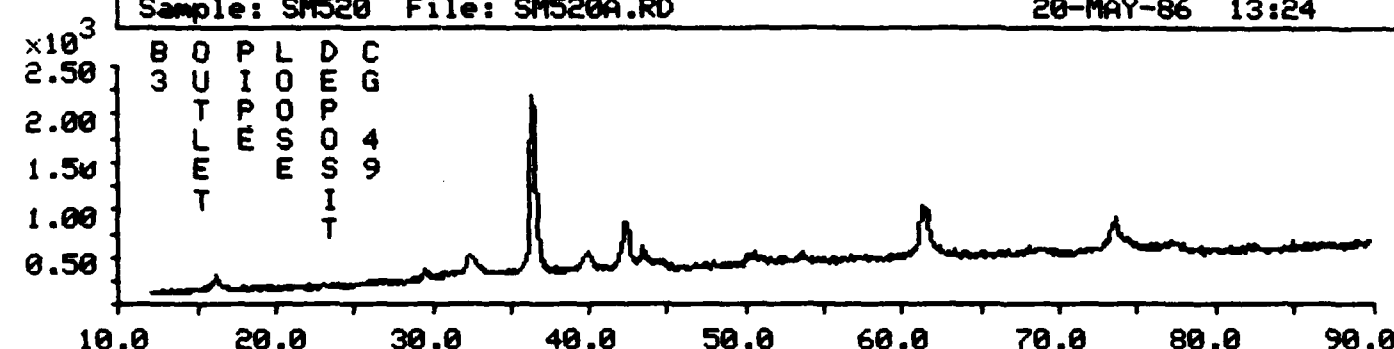
Sample: SM519 File: SM519C.DI

05-JUN-86 15:21

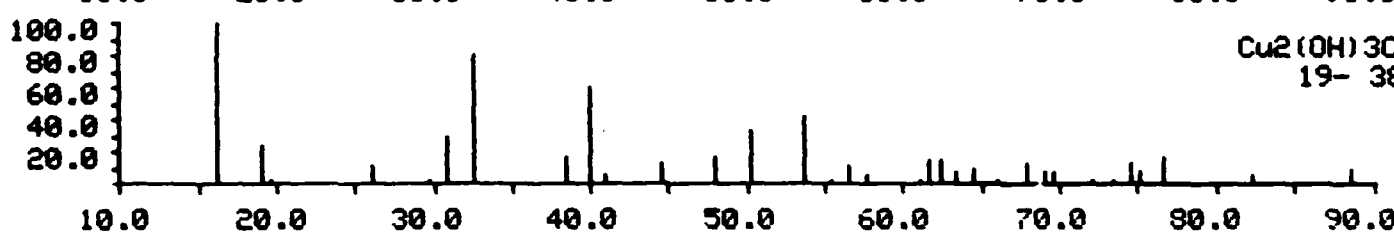


Sample: SM520 File: SM520A.RD

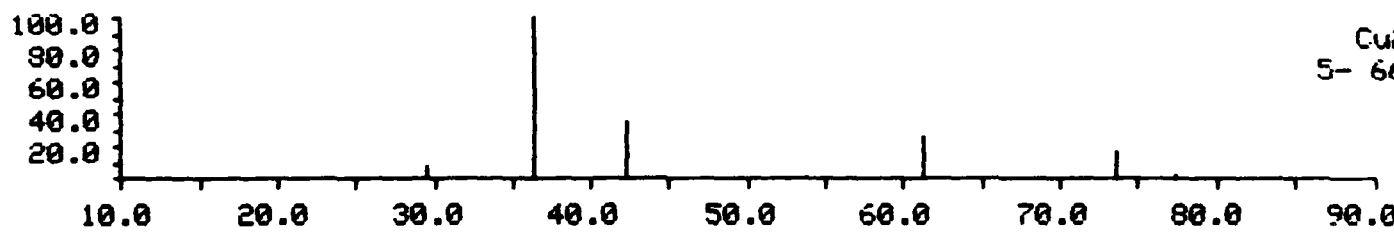
20-MAY-86 13:24



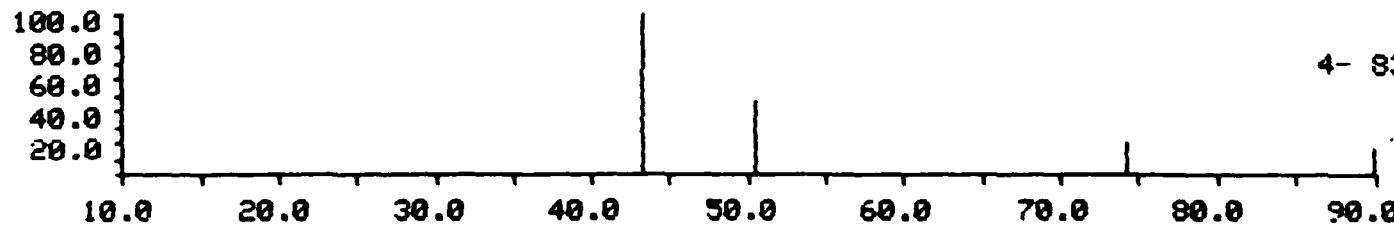
B O P L D C  
3 U I O E G  
T P I O P  
L E S O P  
E F E S O  
T I T 4  
9



Cu<sub>2</sub>(OH)<sub>3</sub>Cl  
19-389



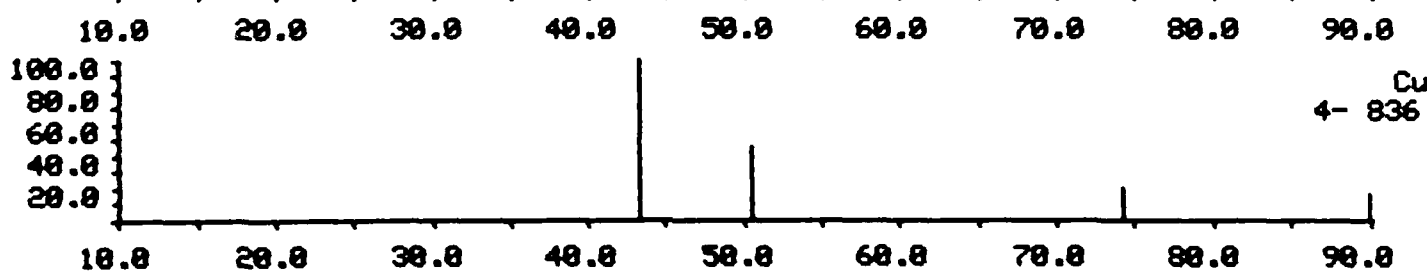
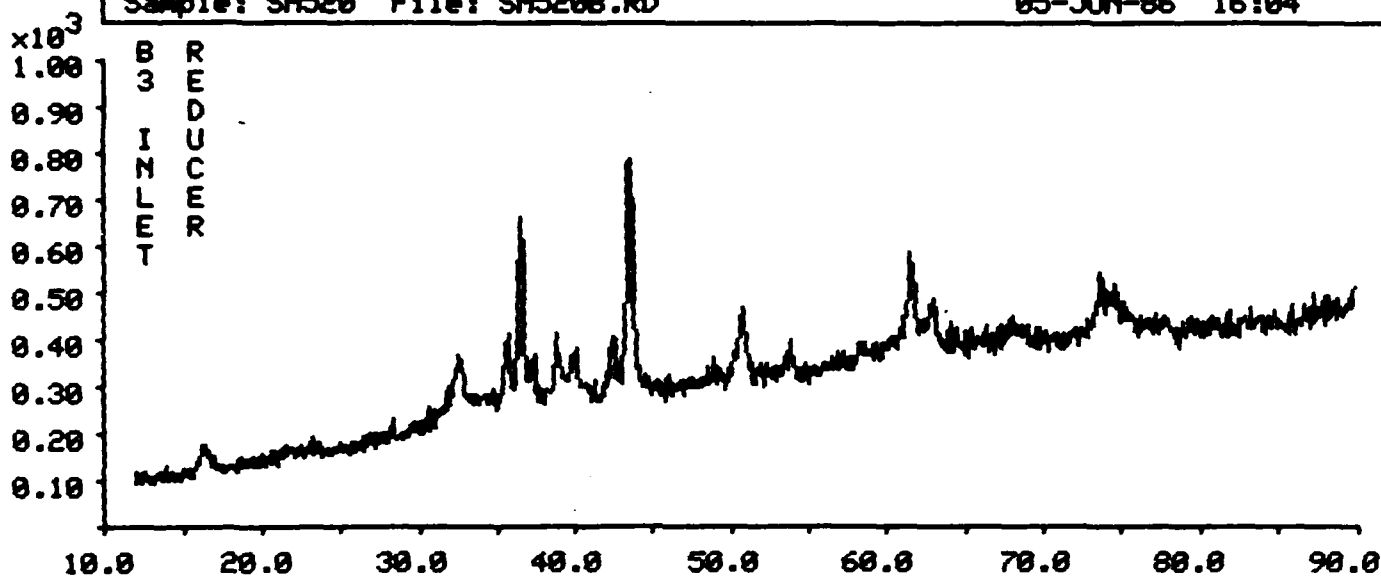
Cu<sub>2</sub>O  
5-667



Cu  
4-836

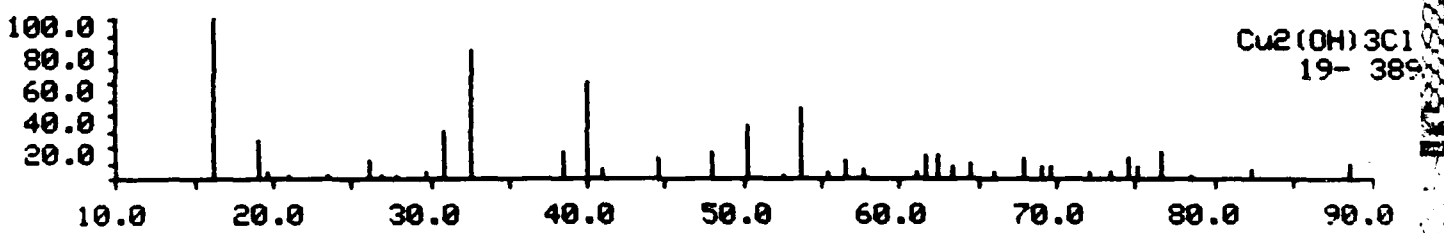
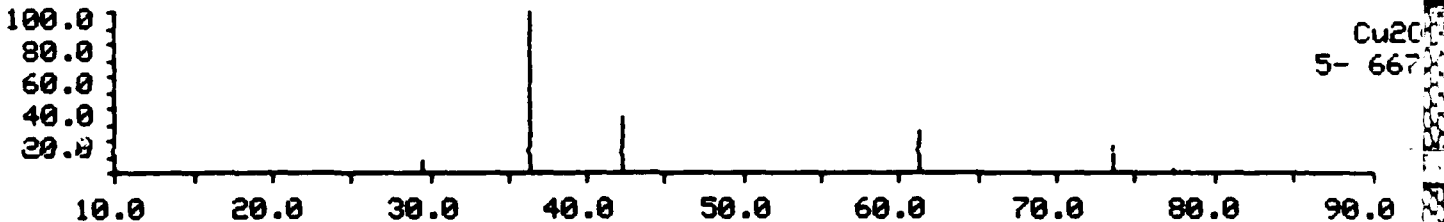
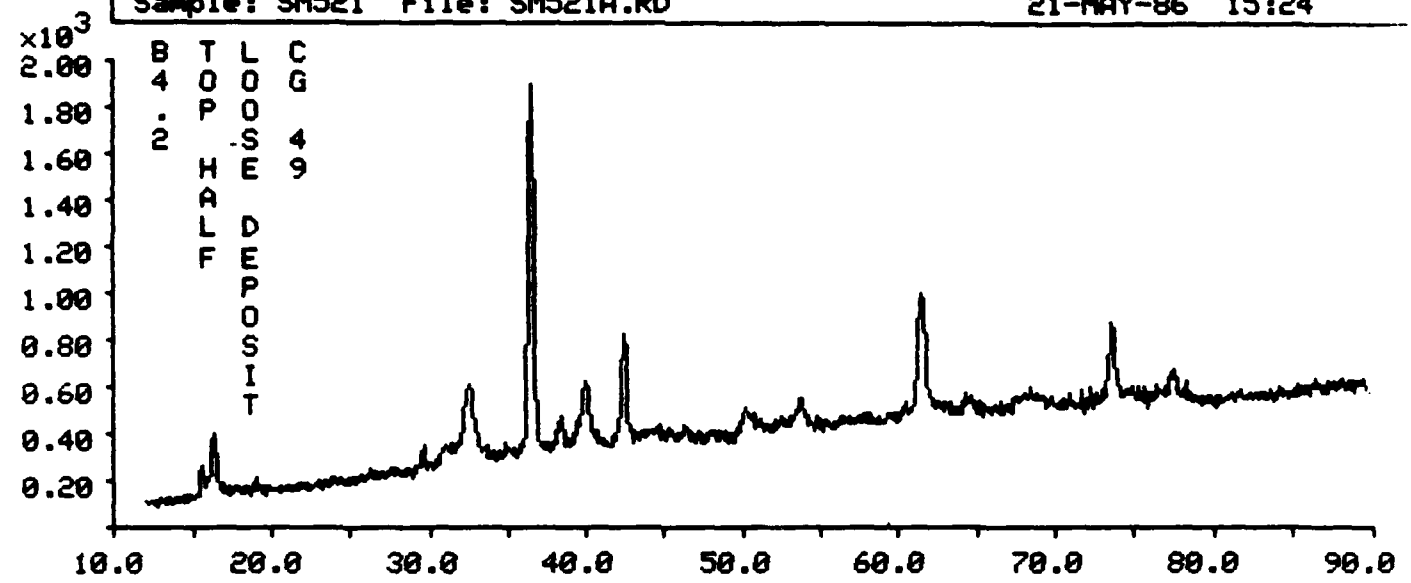
Sample: SM520 File: SM5208.RD

05-JUN-86 16:04



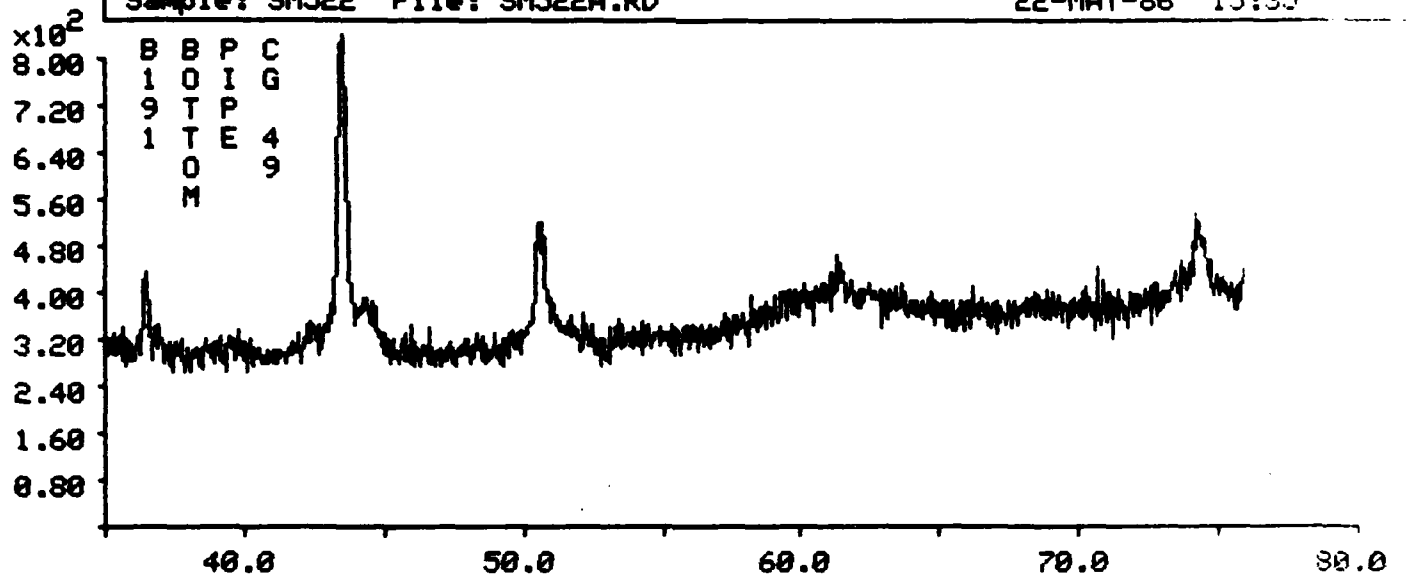
Sample: SM521 File: SM521A.RD

21-MAY-86 15:24

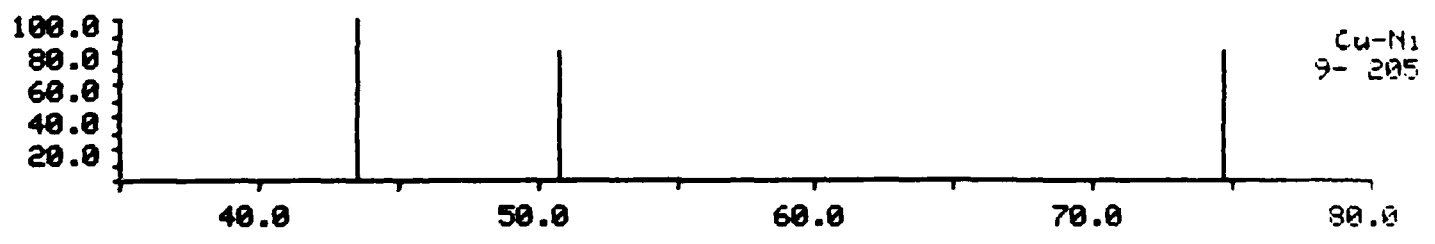
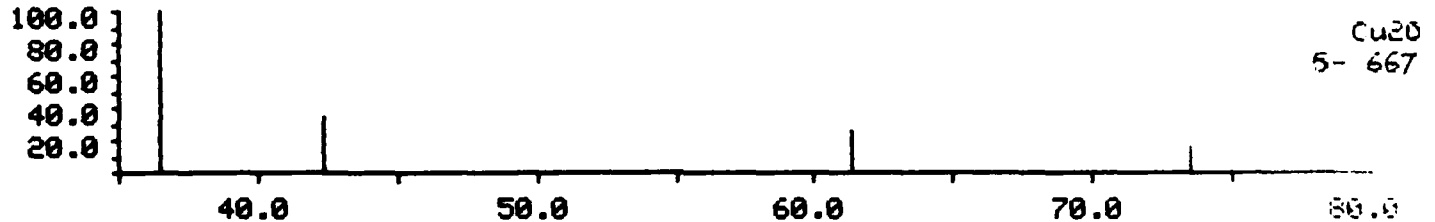


Sample: SM522 File: SM522A.RD

22-MAY-86 15:35

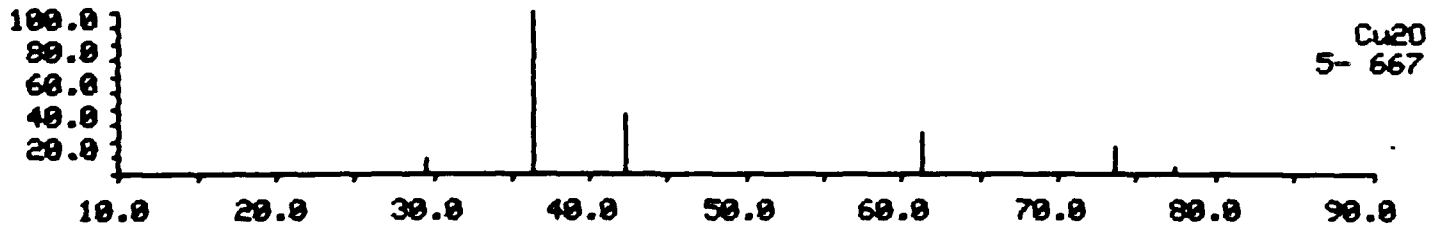
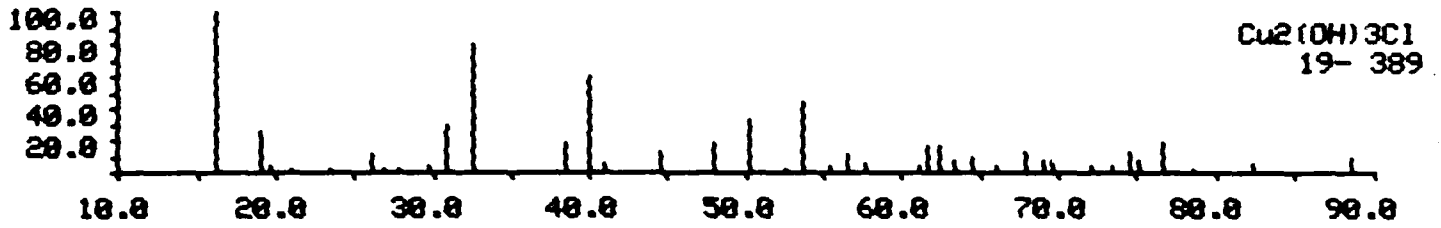
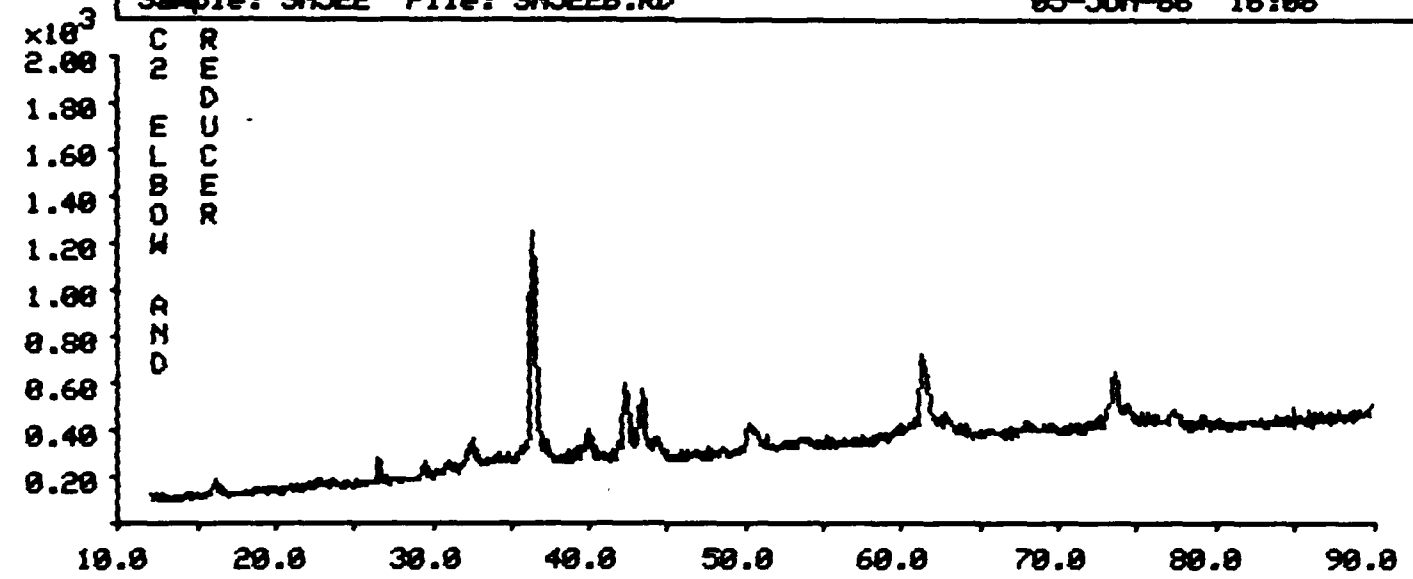


B B P C  
1 0 I G  
9 T P 4  
1 T E 9  
O M



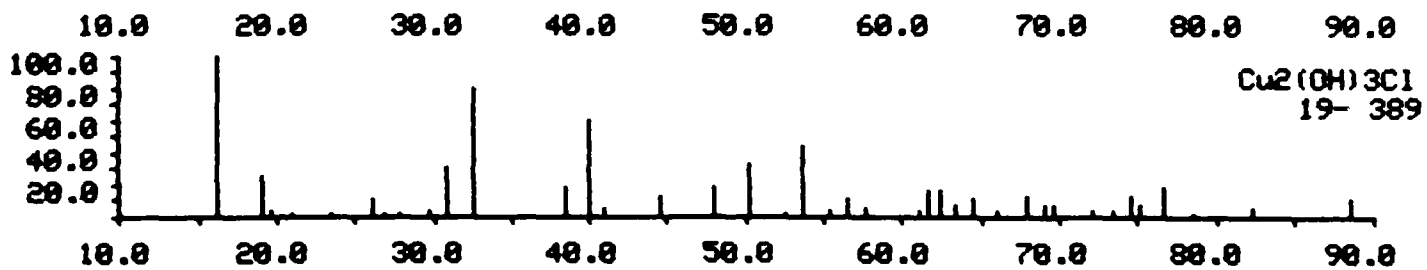
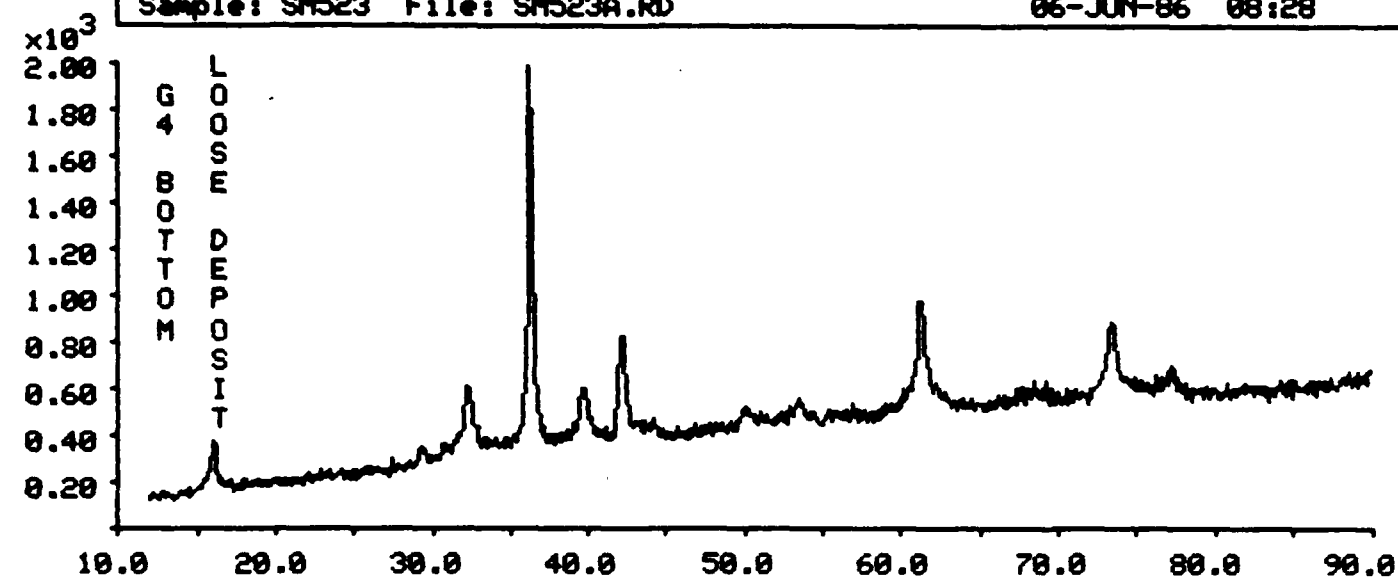
Sample: SM522 File: SM522B.RD

05-JUN-86 16:08



Sample: SM523 File: SM523A.RD

06-JUN-86 08:28





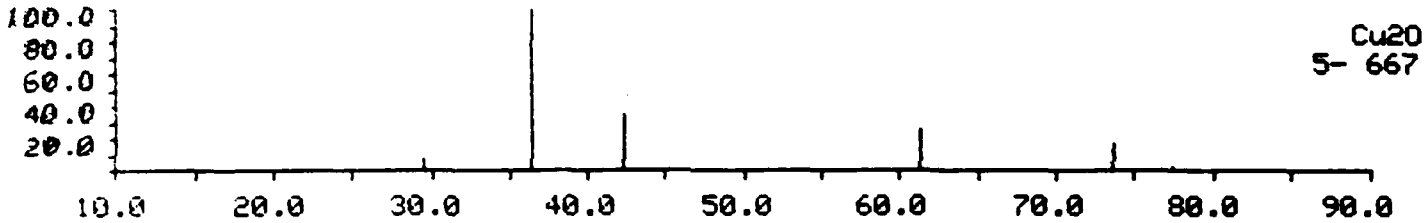
Sample: SM527 File: SM527A.RD

28-MAY-86 10:31

$\times 10^3$



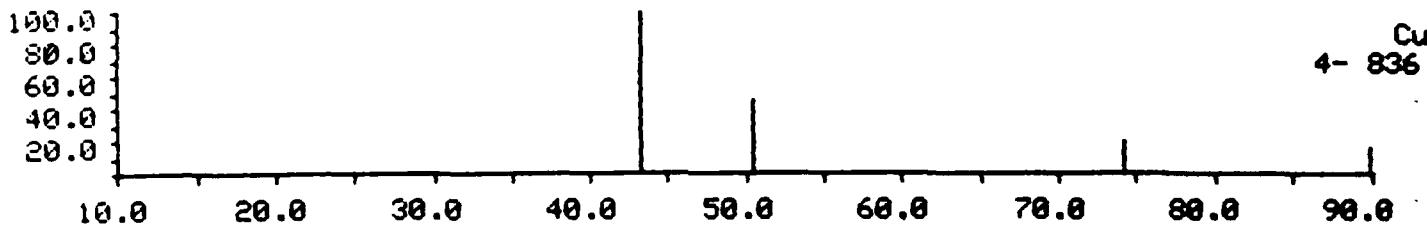
C J P  
G 2 I  
4 1 P  
S E  
T  
O  
P



Cu<sub>2</sub>O  
5- 667



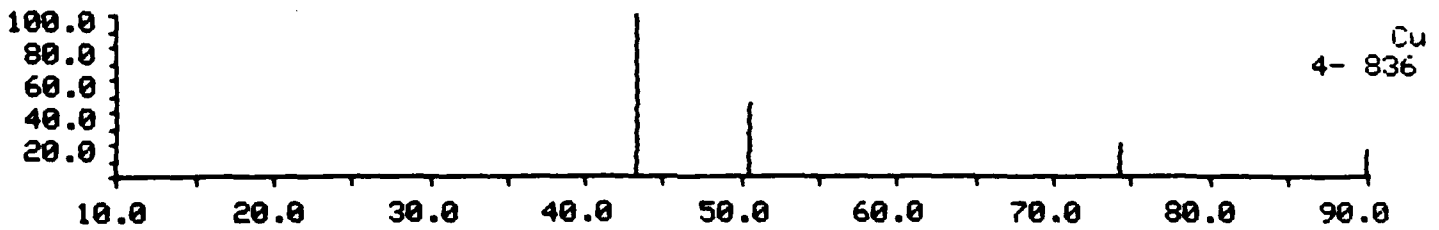
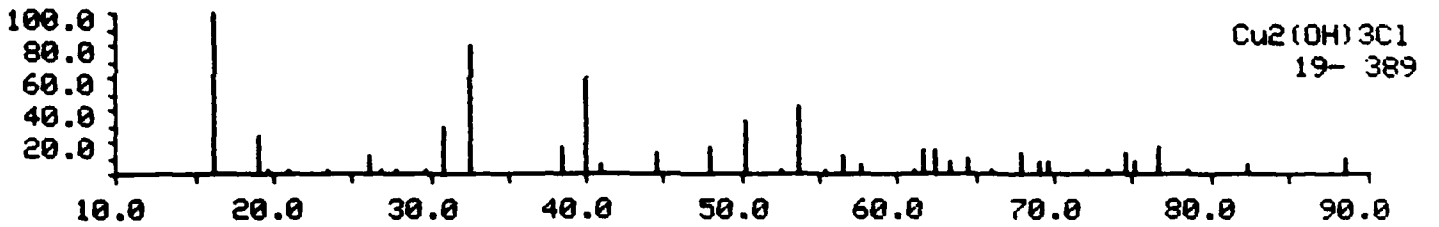
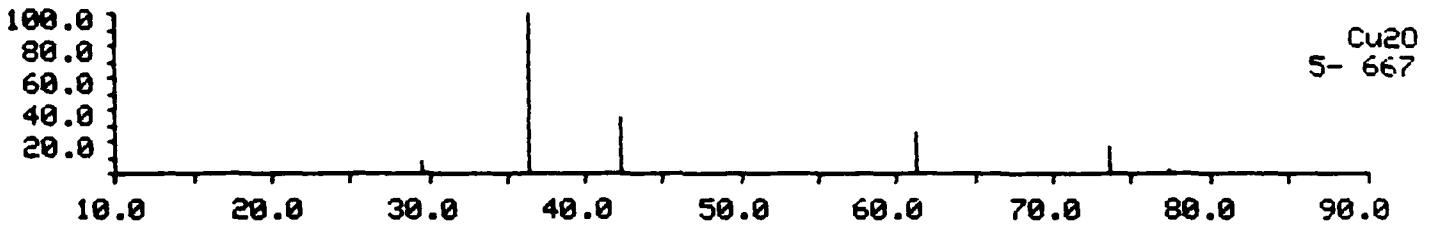
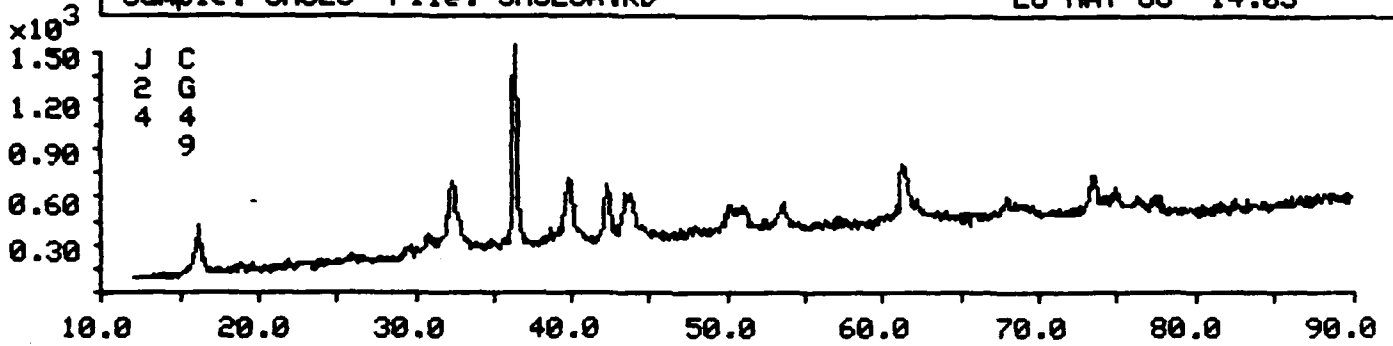
Cu<sub>2</sub>(OH)<sub>3</sub>Cl  
19- 389



Cu  
4- 836

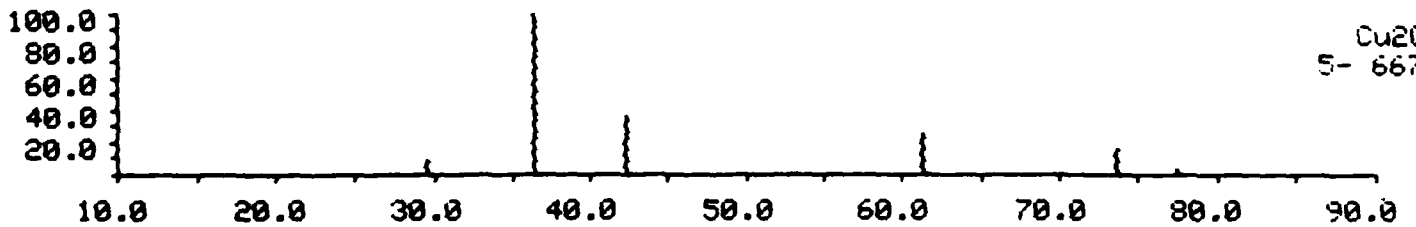
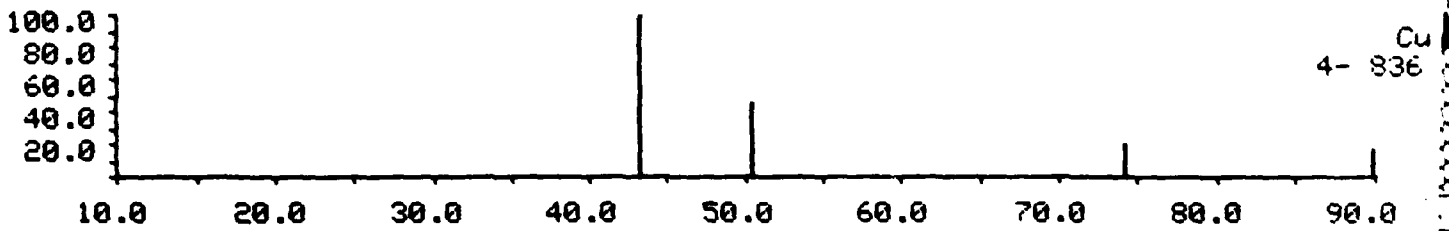
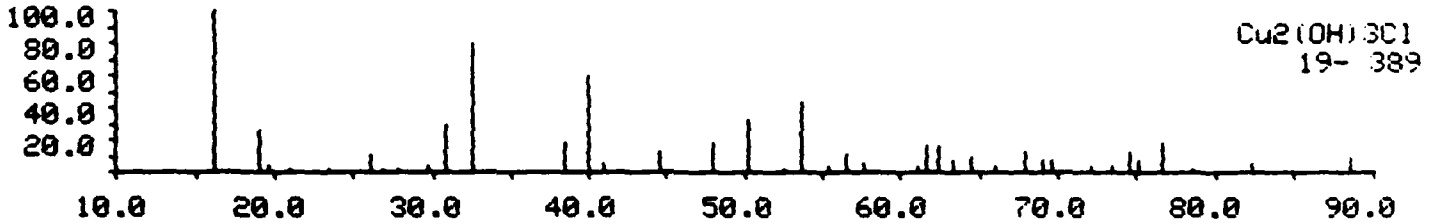
Sample: SM528 File: SM528A.RD

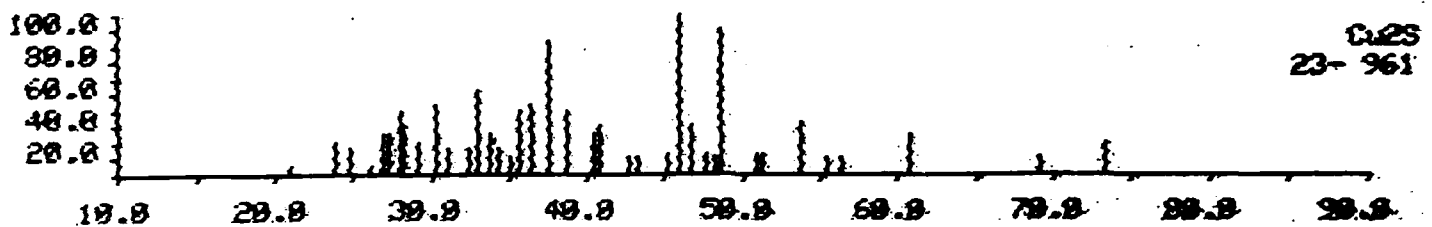
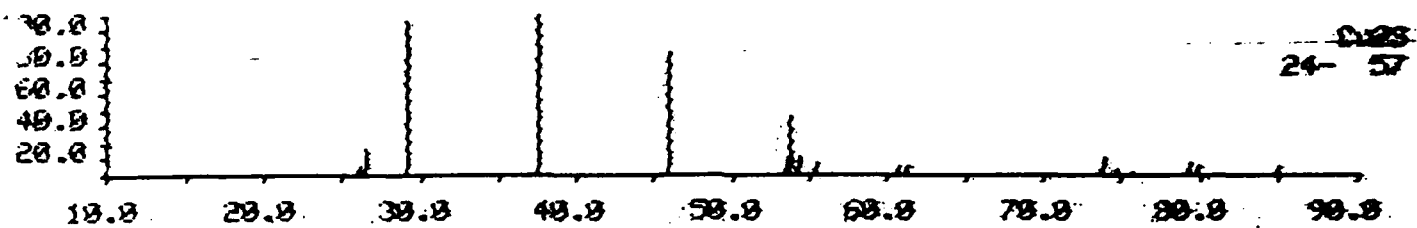
28-MAY-86 14:03



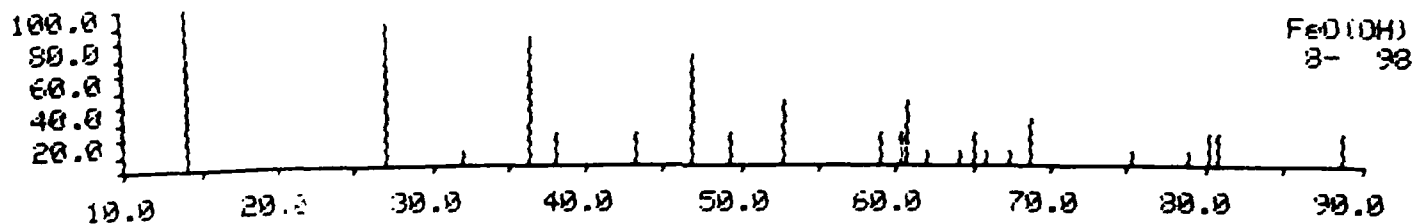
Sample: SM528 File: SM528B.RD

28-MAY-86 14:45





Standard Diffractograms for Forms of Cuprous Sulfide



Standard Diffractogram for Lepidocrocite

**CG-49 SEAWATER PIPING STUDY**  
**PHOTOGRAPHIC DOCUMENTATION**

**Attachment (B)**

**CG-49 SEAWATER PIPING STUDY**  
**PHOTOGRAPHIC DOCUMENTATION**

**Attachment (B)**

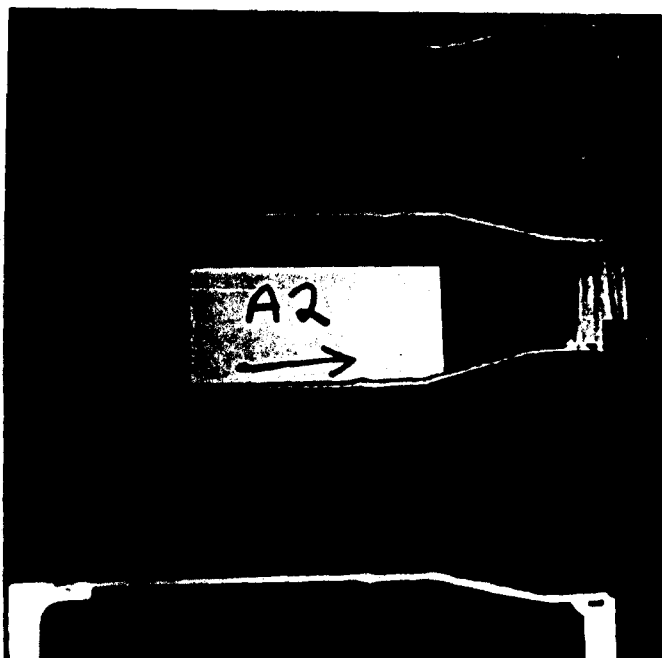
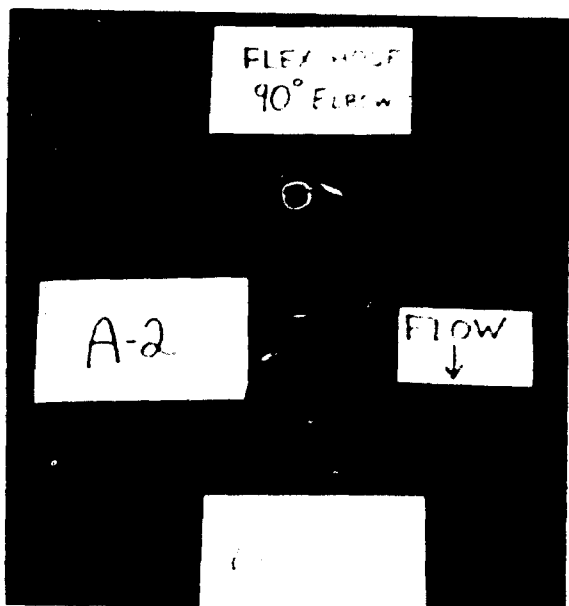


Figure 13: Sample A2, as split.



Figure 14: Sample A2, inlet end.



Figure 15: Sample A2, outlet end.

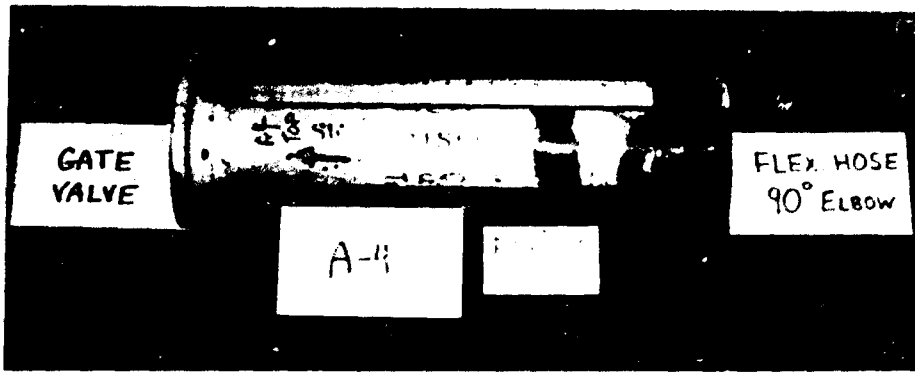


Figure 2a: Sample A4.

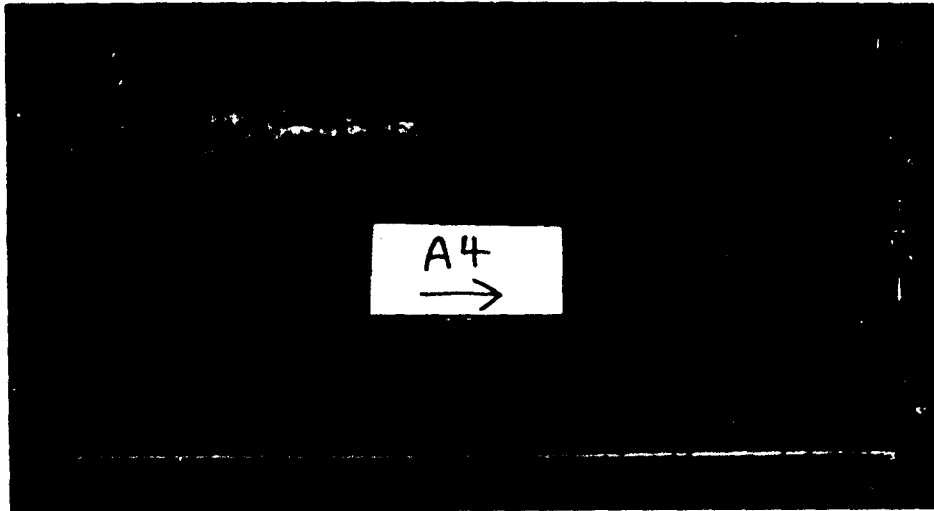


Figure 2b: Sample A4, as split.

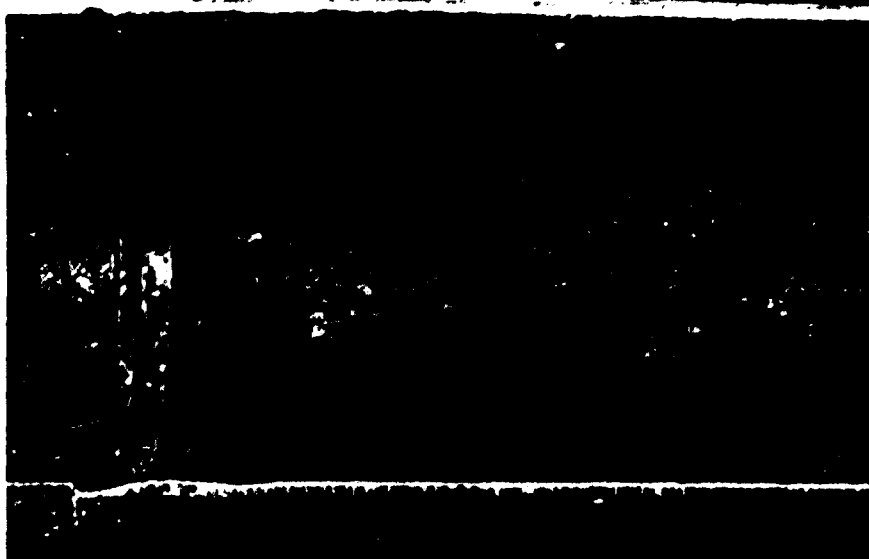


Figure 2c: Sample A4, inlet end, top half.



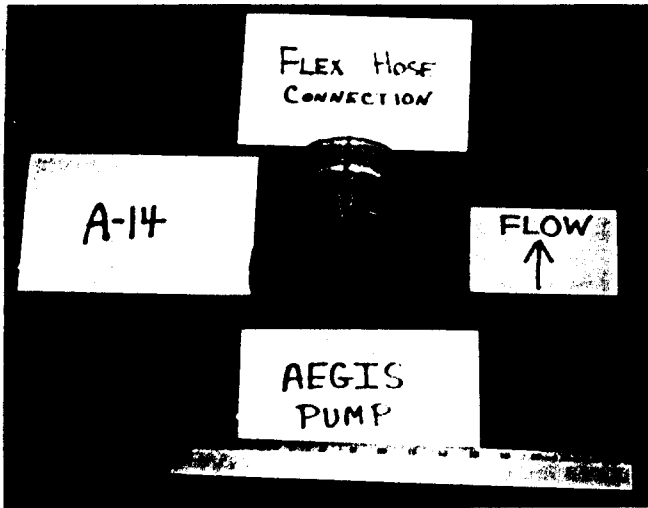


Figure 3: Sample A14.

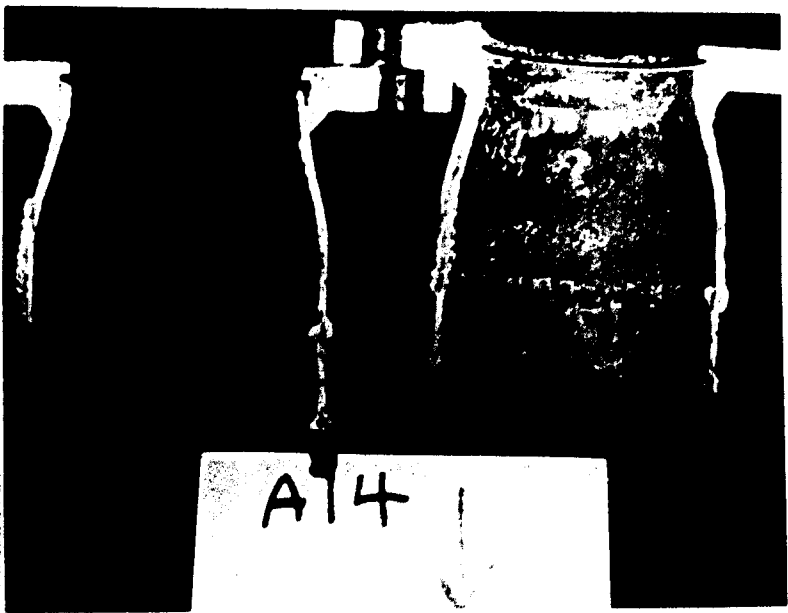


Figure 4: Sample A14.

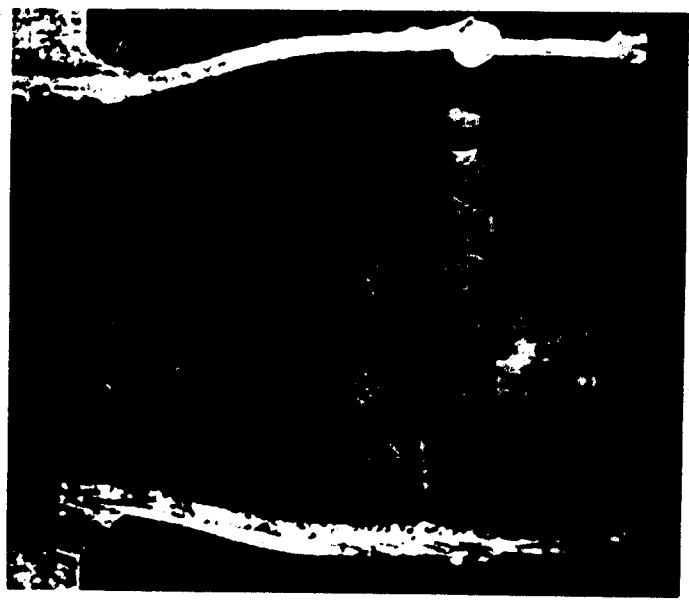


Figure 5: Sample A14.

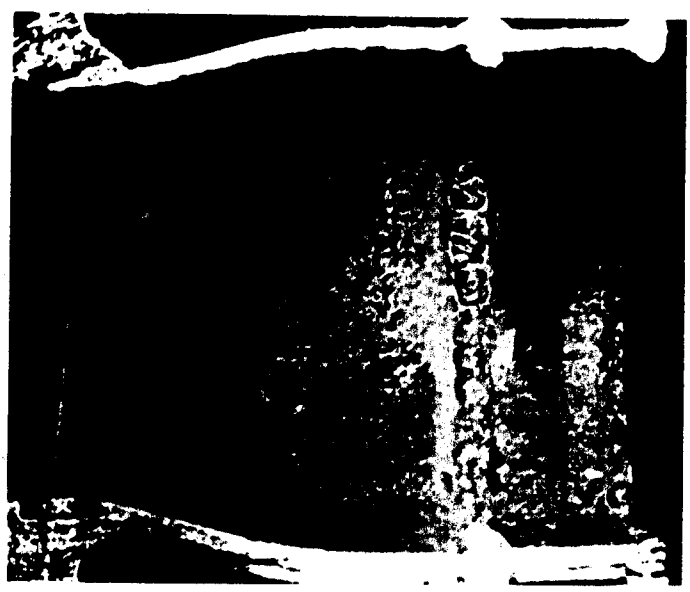


Figure 6: Sample A14.

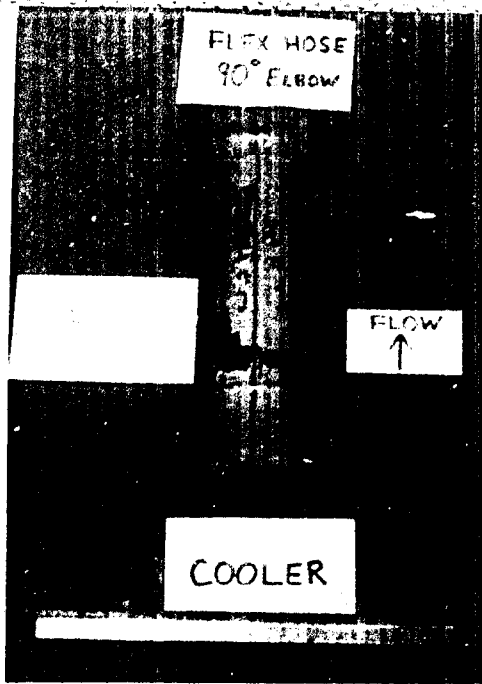


Figure 4a: Sample B3.

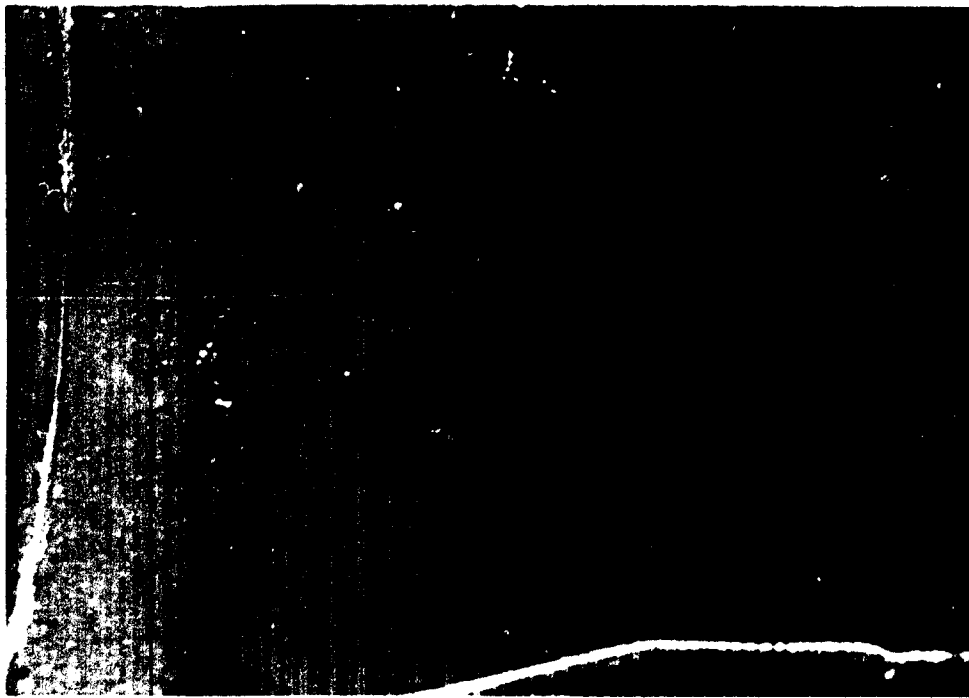


Figure 4b: Sample B3, inlet end. Flow is from left to right.

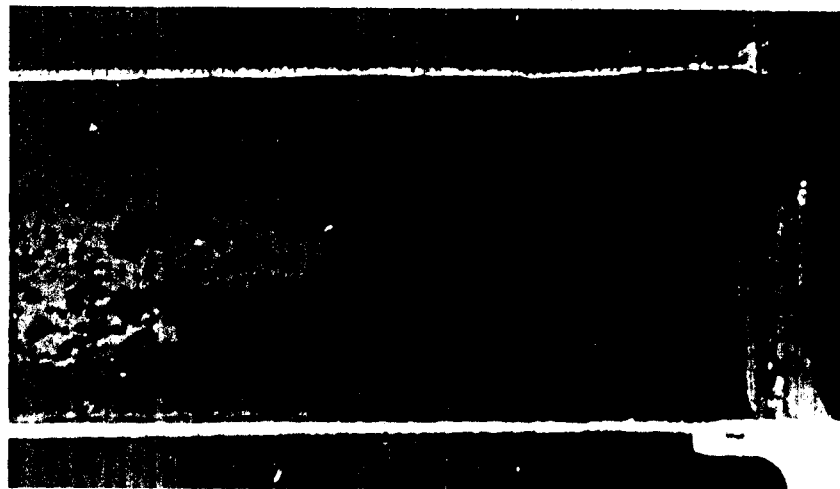


Figure 4c: Sample B3, outlet end. Flow is from left to right.

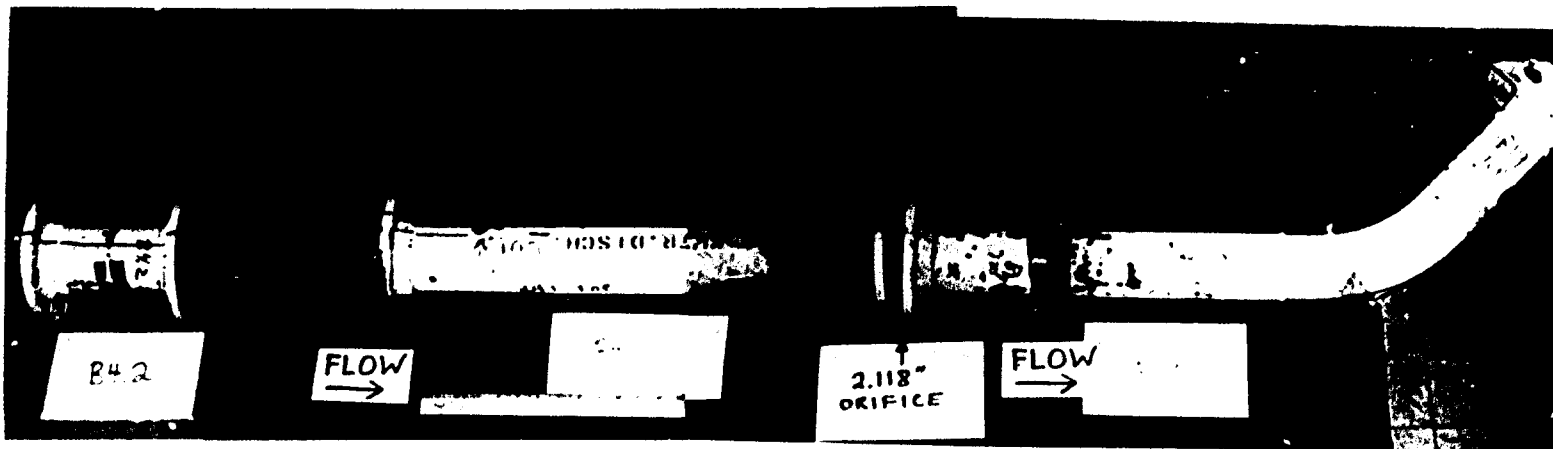


Figure 5a: Samples B4, B19, and flow meter FM1.



Figure 5b: Sample B4.1, inlet end, top half. Flow is from left to right.

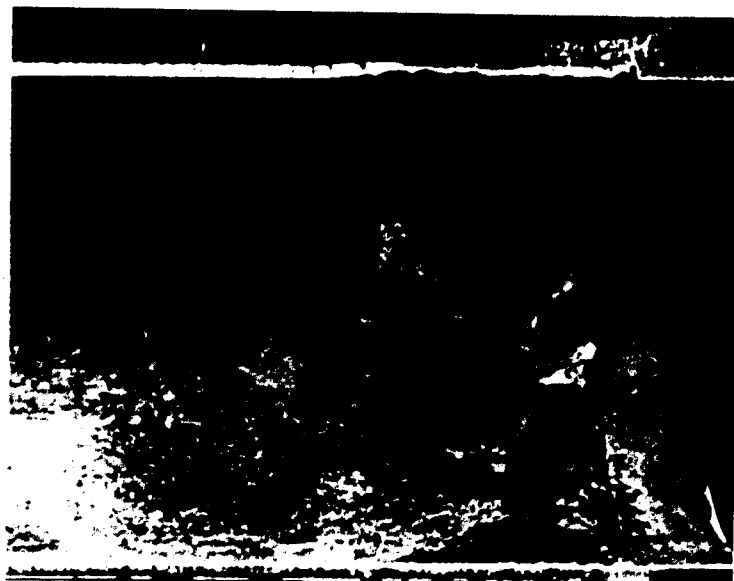


Figure 5c: Sample B4.1, outlet end, bottom half. Flow is from left to right.

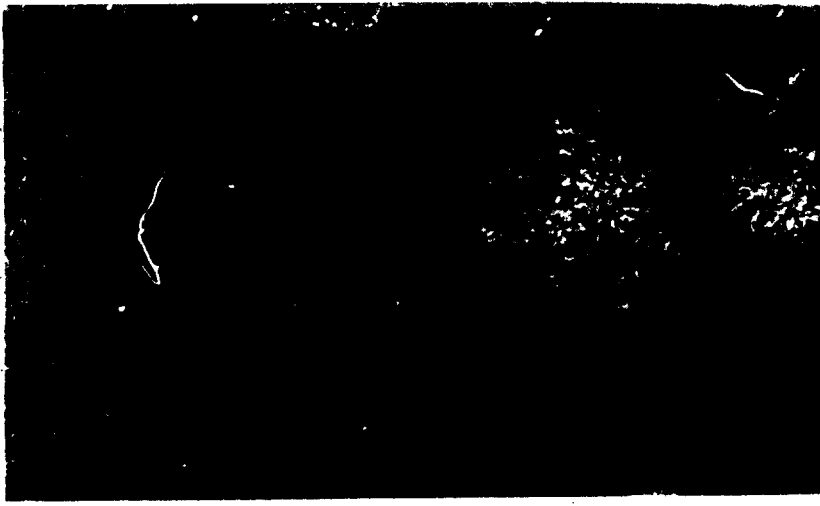


Figure 5d: Sample B4.2, inlet end, top half. Flow is from left to right.

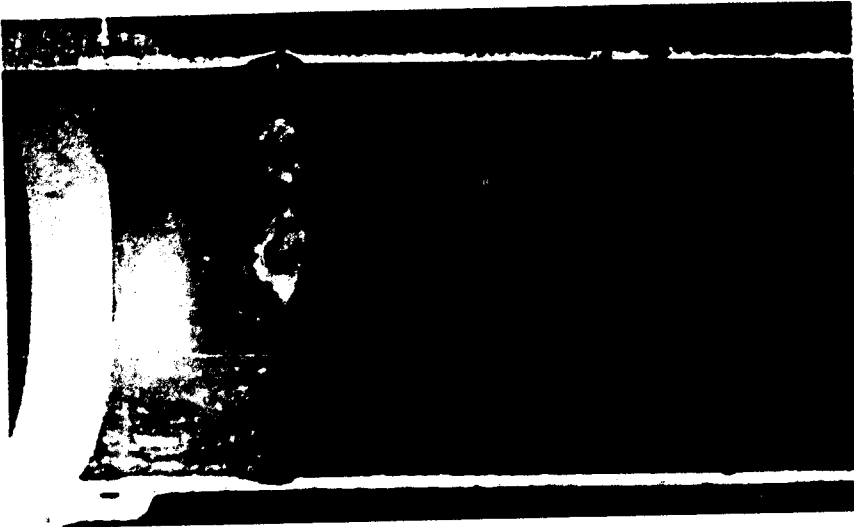


Figure 5e: Sample B19, inlet end, bottom half. Flow is from left to right.

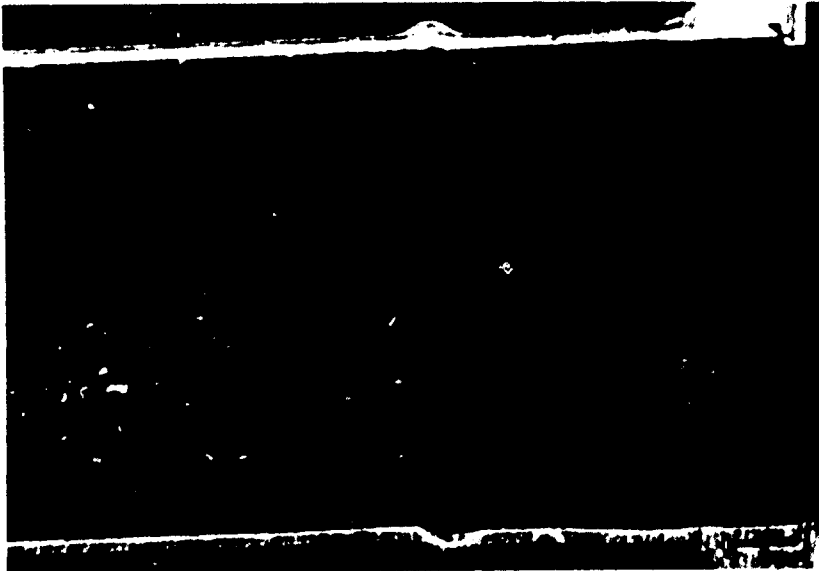


Figure 5f: Sample B19, outlet end, bottom half. Flow is from left to right.

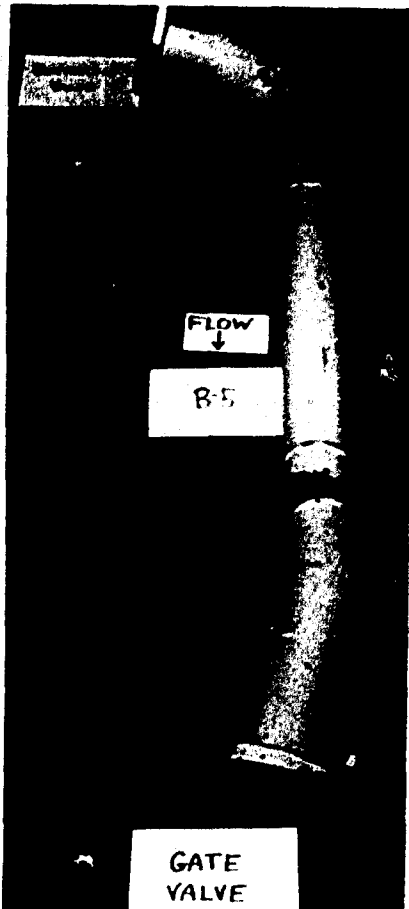


Figure 6a: Sample B5.



Figure 6b: Sample B5, inlet end, as split.

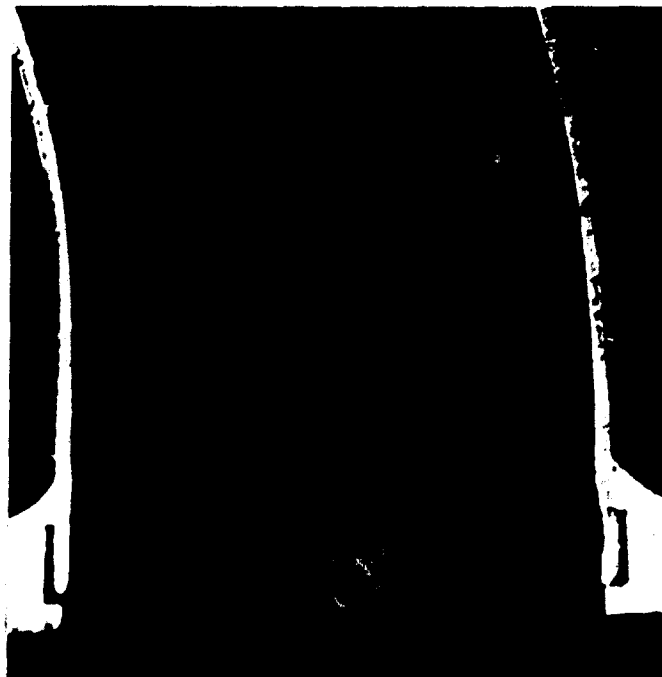


Figure 6c: Sample B5, inlet end.

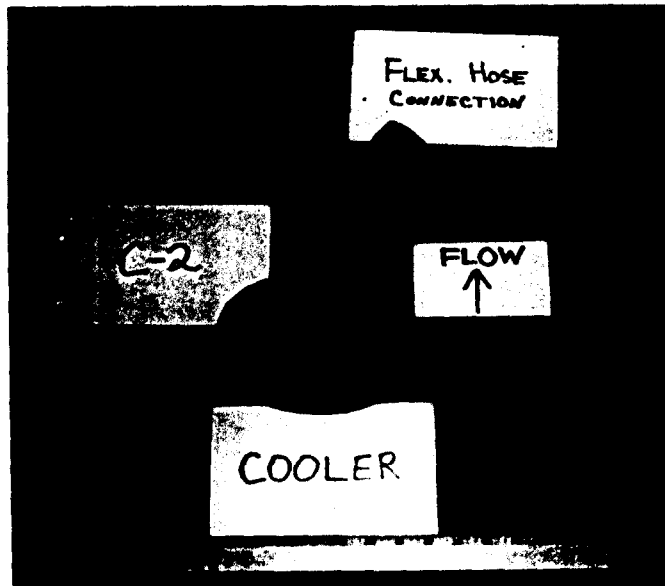


Figure 7a: Sample C2.



Figure 7b: Sample C2, inlet end.

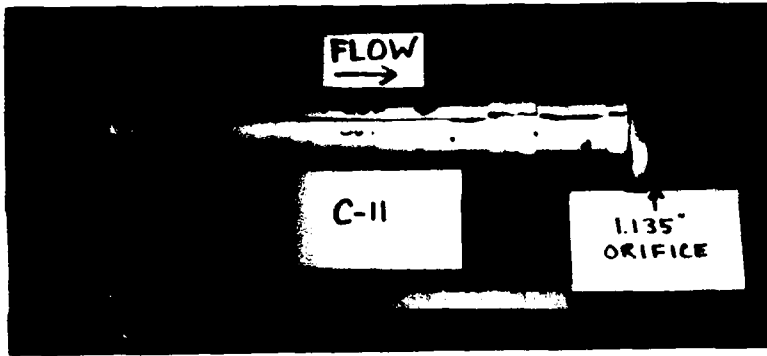


Figure 8a: Sample C11.

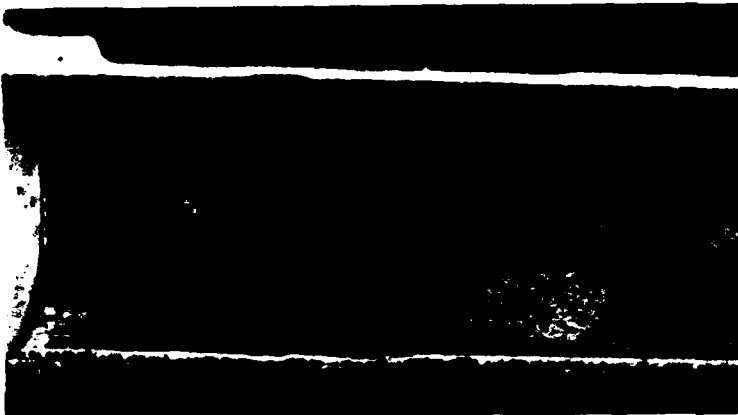


Figure 8b: Sample C11, inlet end, bottom half. Flow is from left to right.

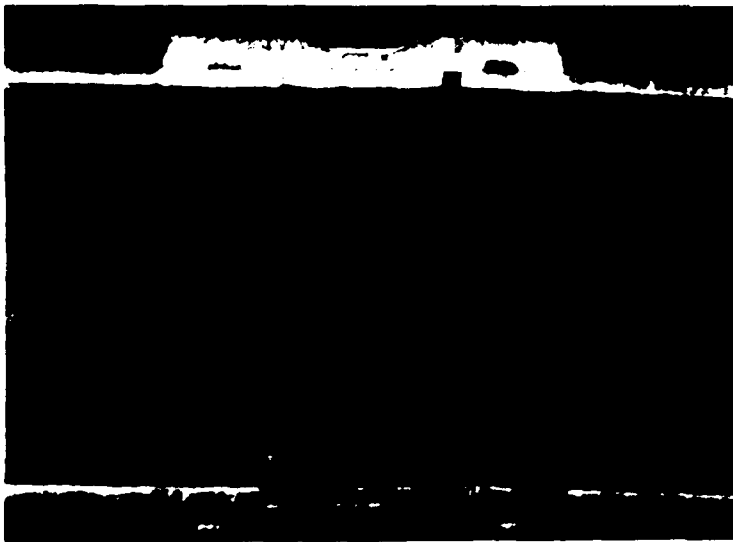


Figure 8c: Sample C11, coupling, bottom half. Flow is from left to right.

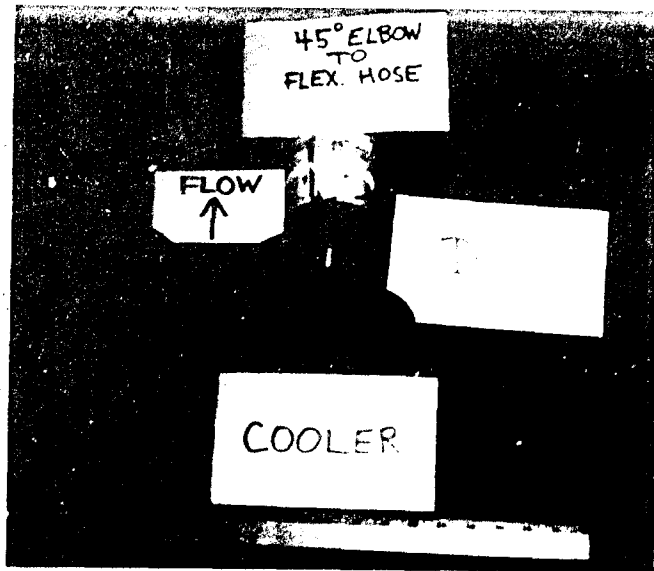


Figure 9a: Sample D1.

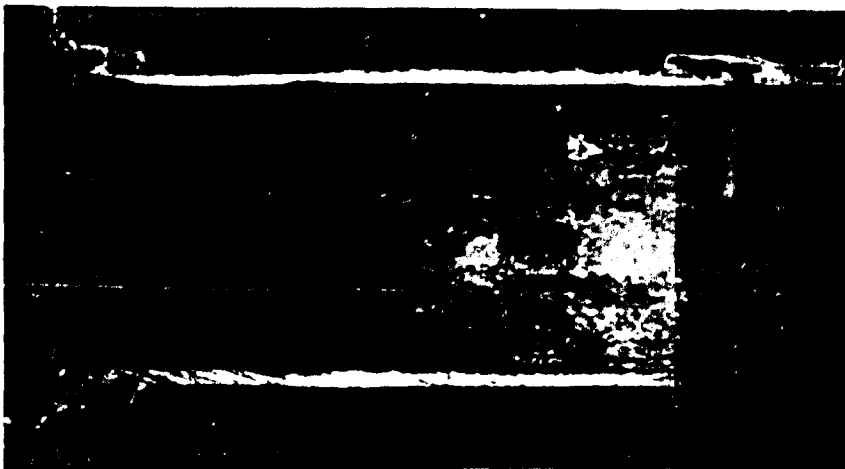


Figure 9b: Sample D1, as split.  
Flow is from left to right.



Figure 9c: Sample D1, inlet  
end. Opening corresponds to  
welded boss. Flow is from left  
to right.



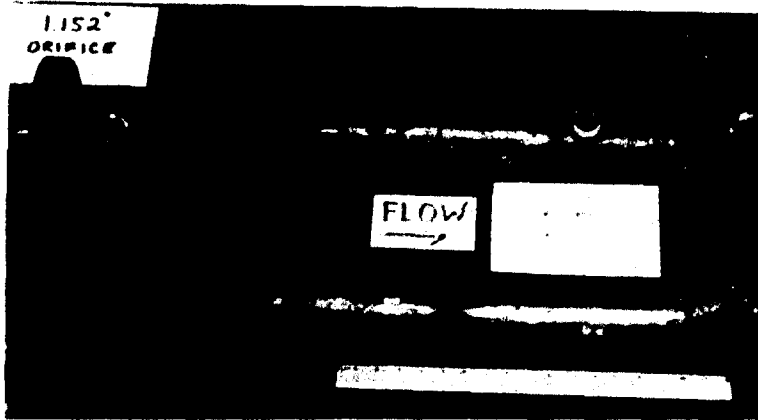


Figure 10a: Sample flow

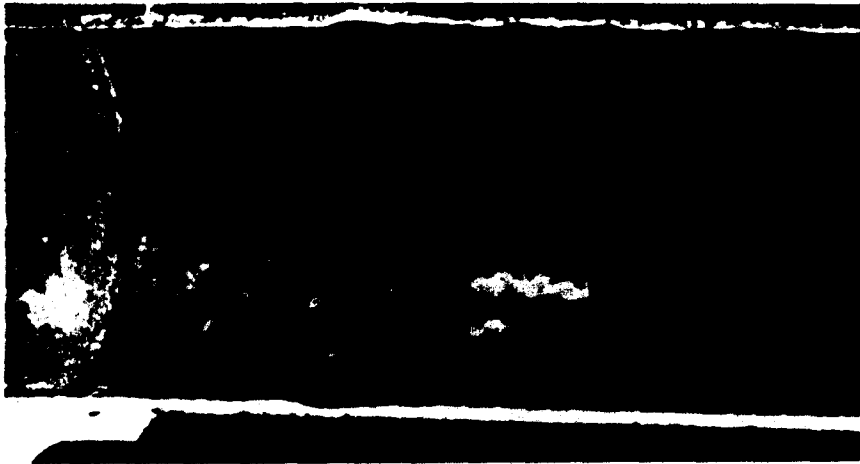


Figure 11: Turbulent flow  
End. Flow is from left to  
right



Figure 12: Turbulent flow  
Flow is from left to right

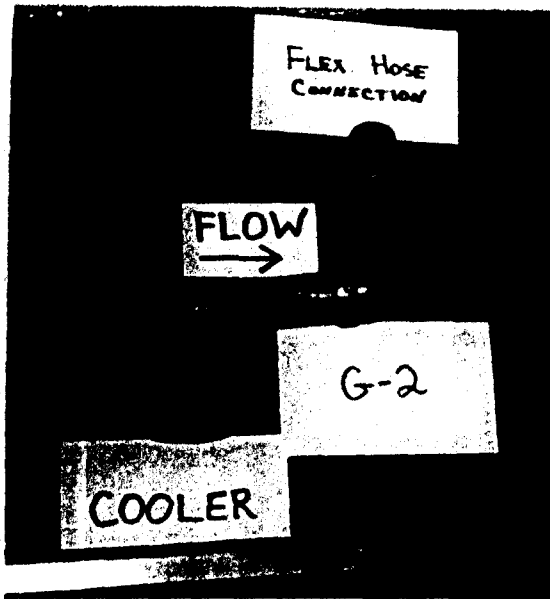


Figure 11a: Sample G2.

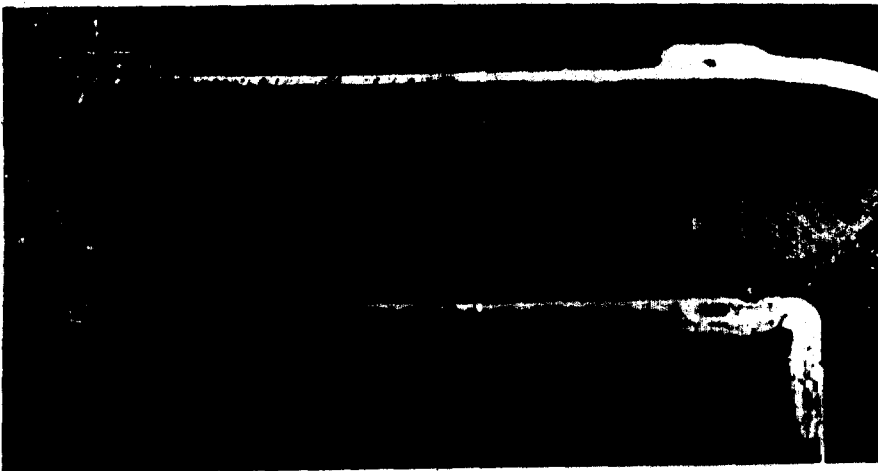


Figure 11b: Sample G2, top half. Flow is from left to right.

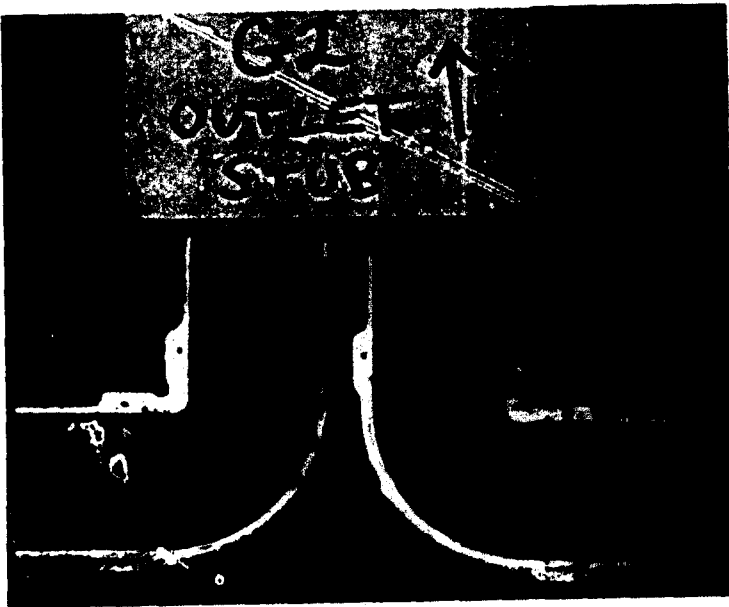


Figure 11c: Sample G2, outlet end.

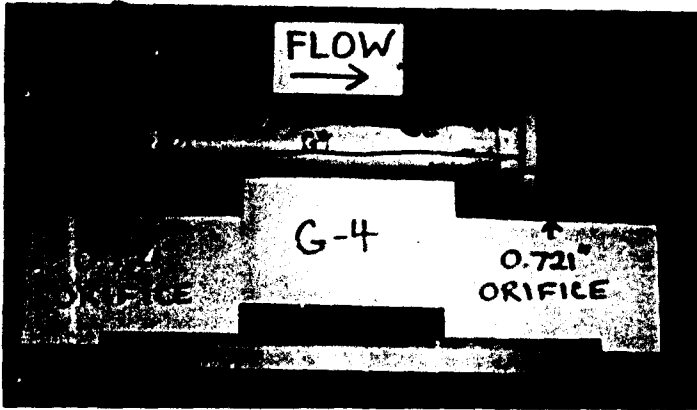


Figure 12a: Sample 04.

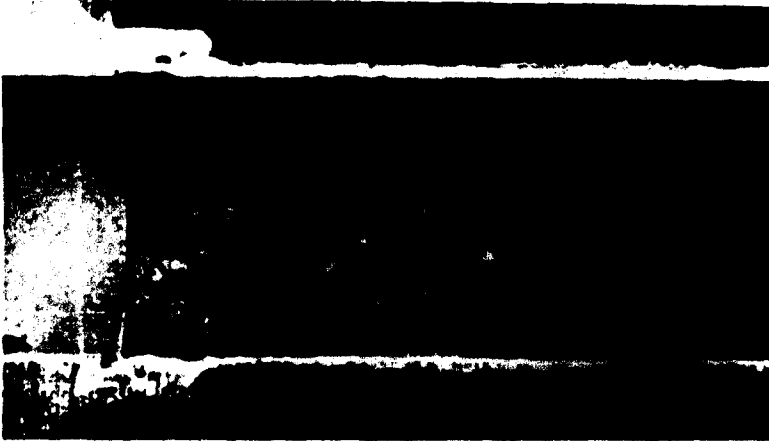


Figure 12b: Sample 04, inlet end, top half. Flow is from left to right.



Figure 12c: Sample 04, outlet end, top half. Flow is from left to right.

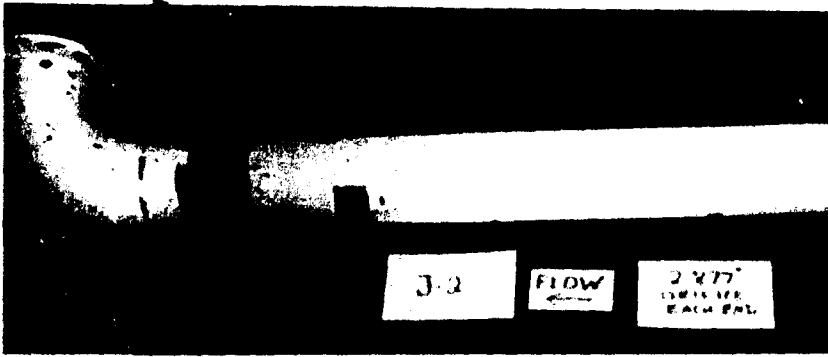


Figure 13a: Sample J1.



Figure 13b: Sample J1, inlet end, as split. Flow is from left to right.

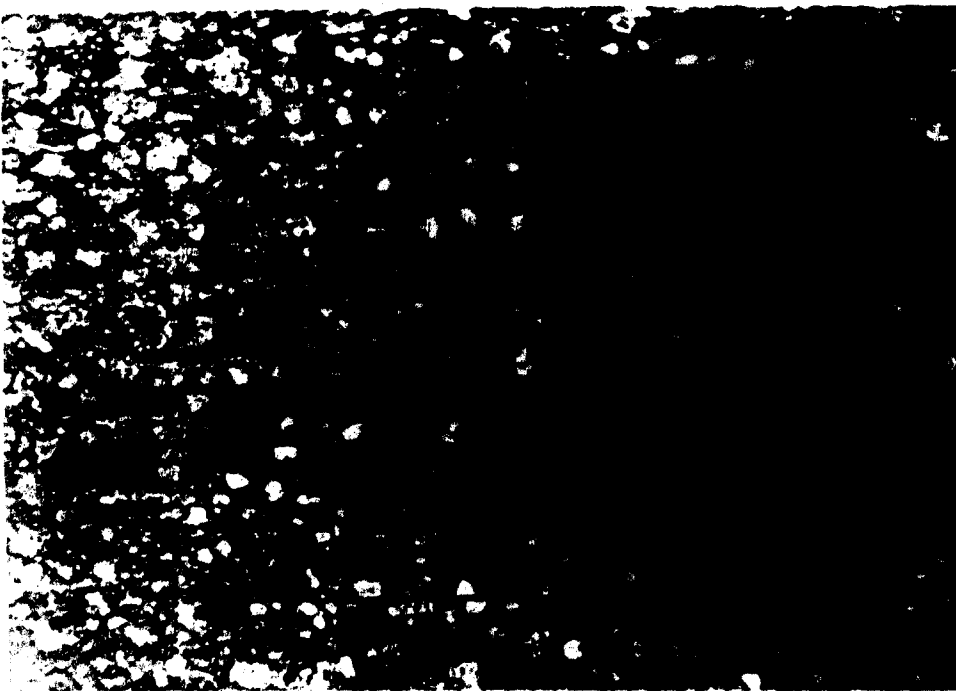


Figure 13c: Sample J2, approx. 6 inches from inlet. Flow is from left to right.

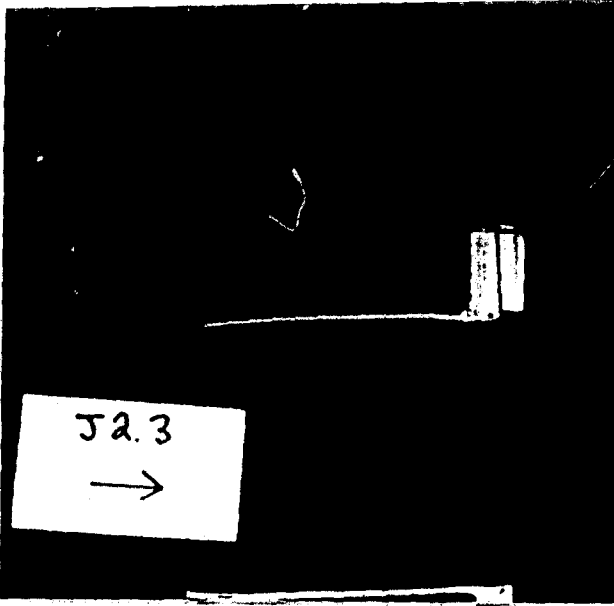


Figure 13d: Sample J2, outlet end.



Figure 13e: Sample J2, outlet end at inside radius of bend.



Figure 13f: Sample J2, outlet end at inside radius of bend.



Figure 14a: Sample from forward AEGIS pump room. Flow is from left to right. Note patch at inlet. Butterfly valve was located immediately adjacent to inlet.



Figure 14b: Sample from forward AEGIS pump room, as split.

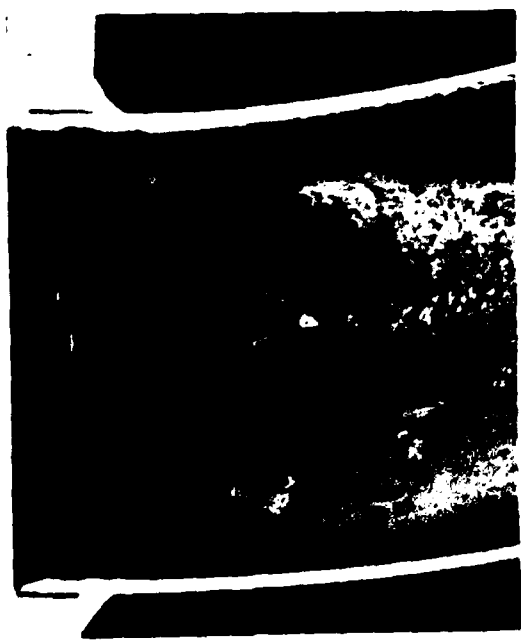


Figure 14c: Sample from forward AEGIS pump room, inlet end. Flow is from left to right.

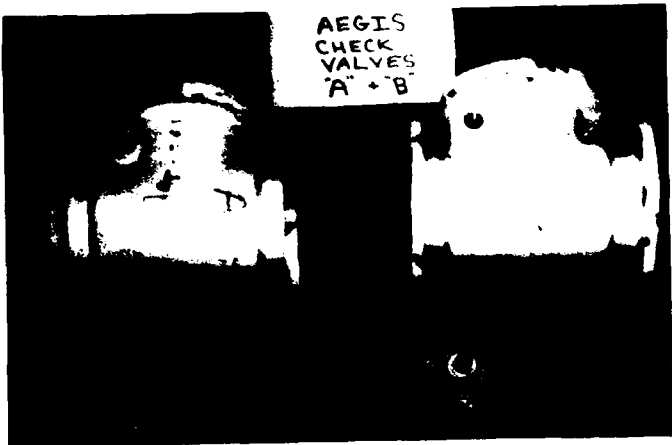


Figure 15: Check valves from AEGIS piping system.

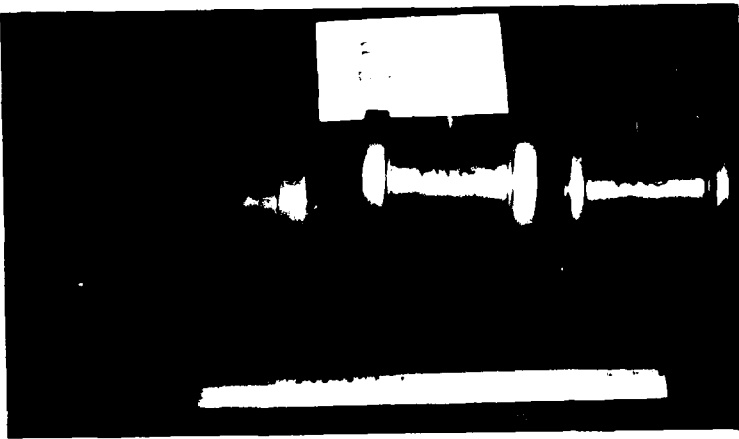


Figure 16a: Flow meters. FM1 is from the att. AEGIS system (see figure 14a); FM2 is from the #1-4 system and FM3 is from the #1 HEAC system.

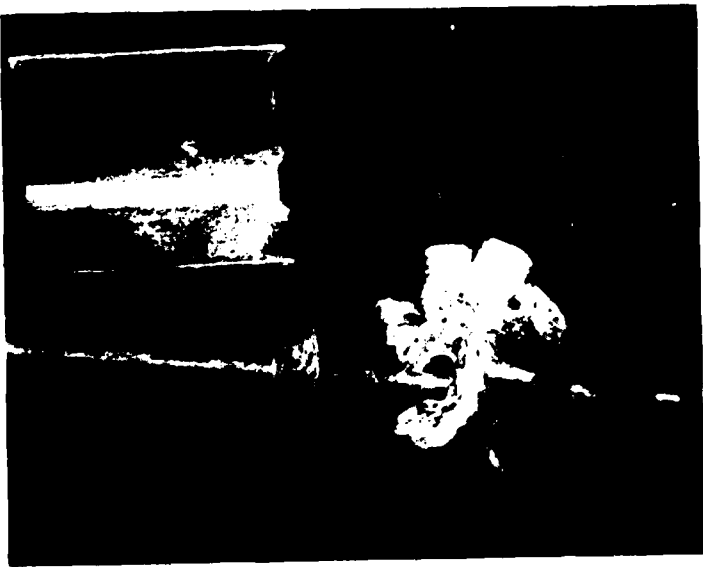


Figure 16b: Internal piping with FM1.

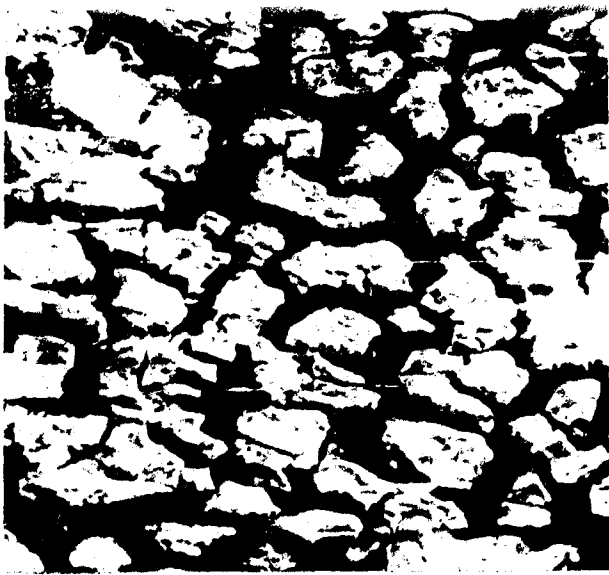


Figure 20: Sample 80, SEM view of surface of black deposit on pipe. MAGNIFICATION: 500X.

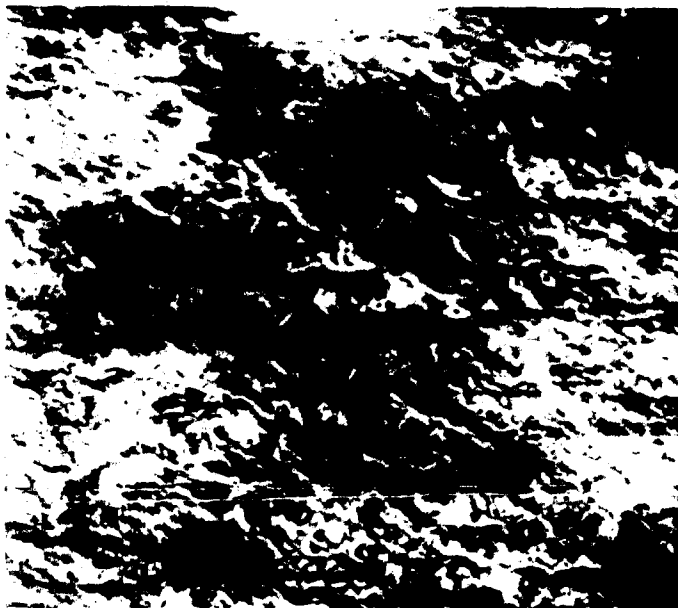


Figure 21: Sample 83, SEM view of surface of red/brown deposit on pipe. MAGNIFICATION: 520X.



Figure 22: Sample 86, cross-section of attack in reducer. Flow is from right to left. MAGNIFICATION: 200X.



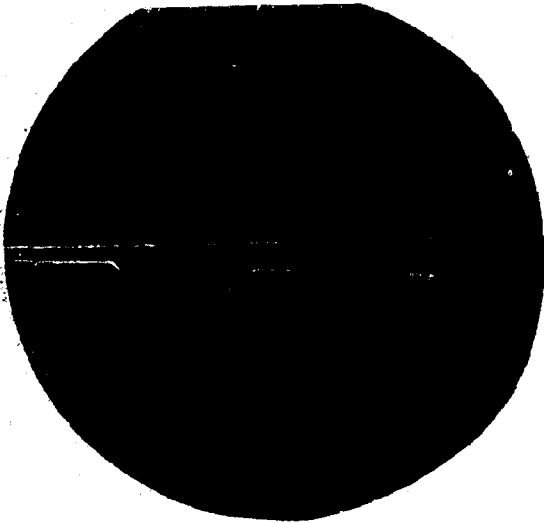


Figure 17: Sample A14, longitudinal section through weld between reducer and pipe. Flow is from right to left. MAGNIFICATION: 30X.

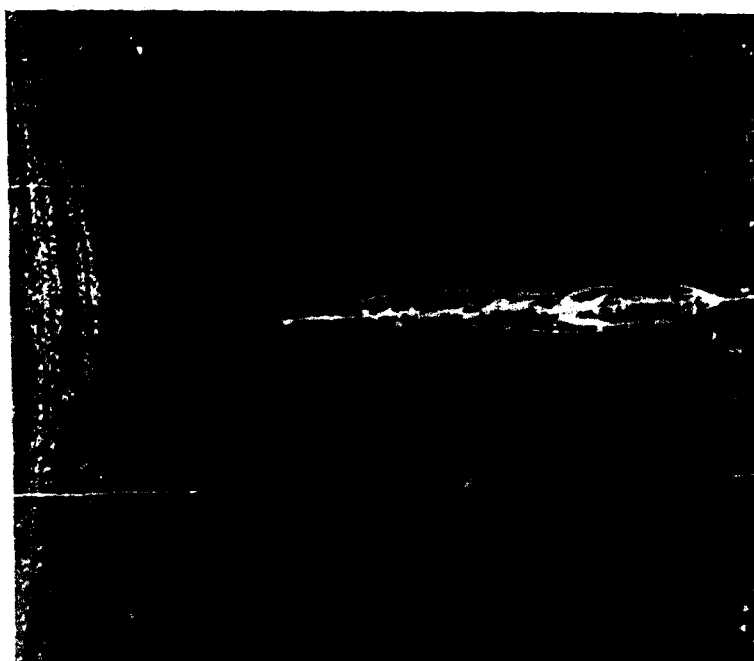


Figure 18: Sample B3, view of damaged area on reducer. Flow is from right to left. MAGNIFICATION: 3X.



Figure 19: Sample B4, view of speckled deposit and small pits in pipe. Flow is from right to left. MAGNIFICATION: 3X.

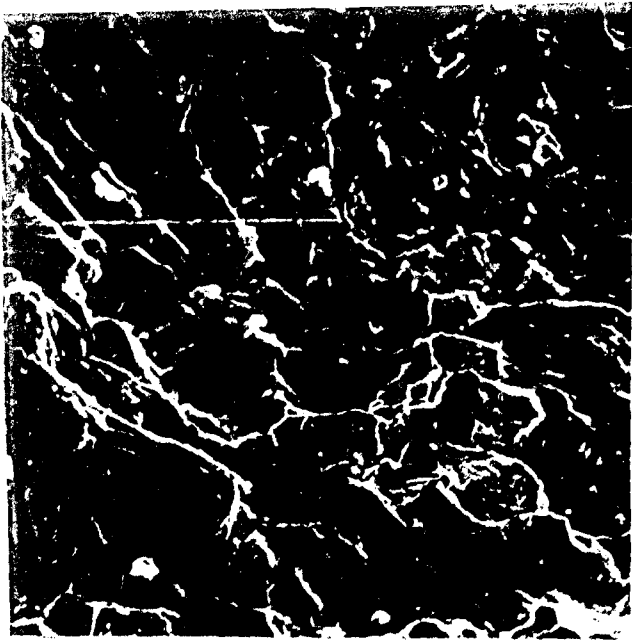


Figure 23: Sample B4.2, SEM view of surface of pipe under flake of black deposit. MAGNIFICATION: 480X.



Figure 24: Sample B4.2, SEM view of deposit on pipe adjacent to outlet flange. MAGNIFICATION: 60X.

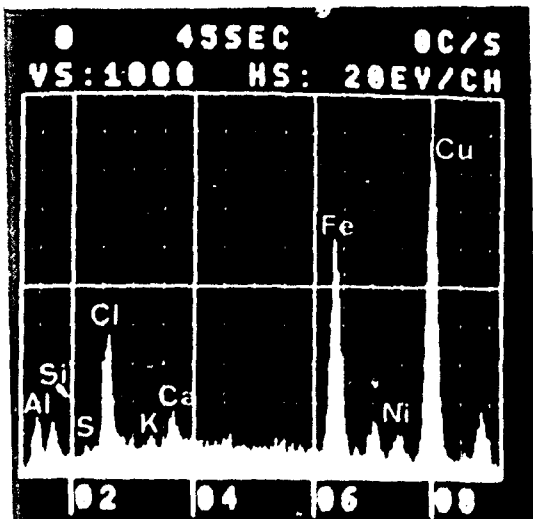


Figure 25: Sample B4.2, EDXA spectrum of element in deposit shown above.

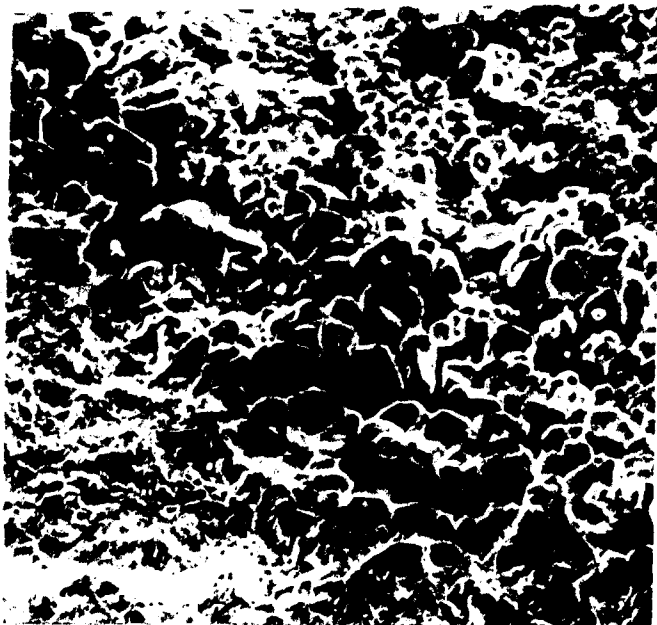


Figure 26: Sample G2, SEM view of the maroon/purple underside of a flake of deposit. Typical of many samples, deposit is mainly copper.  
MAGNIFICATION: 600X.

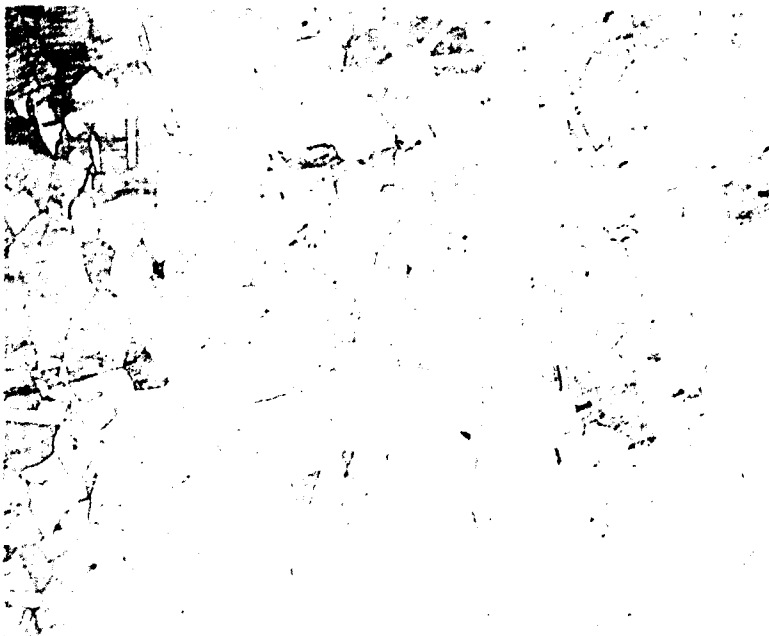


Figure 27: Sample B4.2, photograph of typical microstructure in non-HAZ. This grain structure is considered normal, and is representative of all samples.  
MAGNIFICATION: 200X.

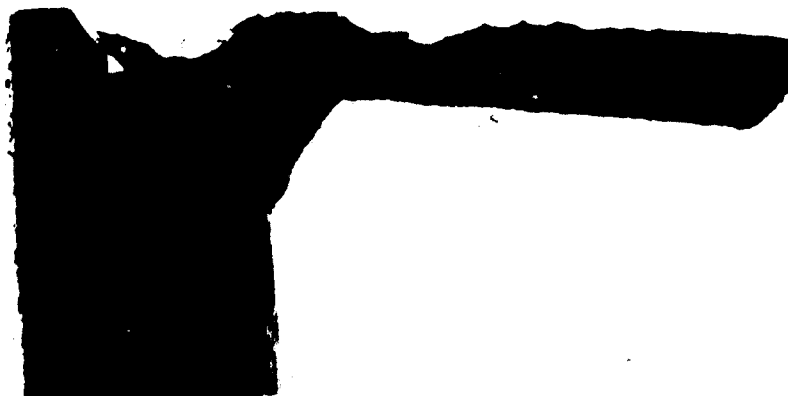


Figure 28: Sample J2, section through weld and flange at outlet end of pipe. Flow is from right to left.  
MAGNIFICATION: 2X.

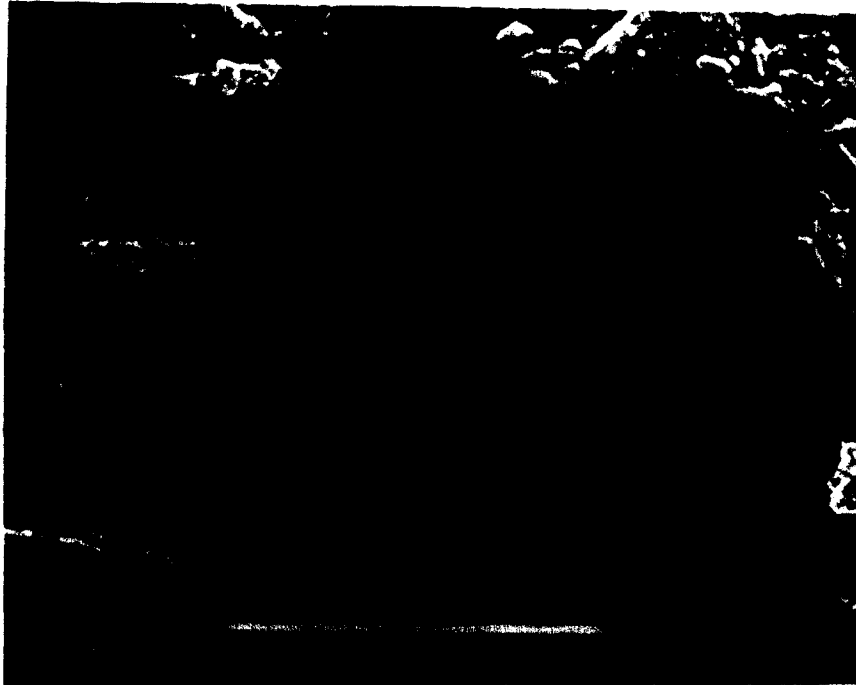


Figure 29: Sample J2, SEM view of bacteria on surface of pipe near inlet end.



Figure 30: Sample J2, end section of pipe with deposit. This deposit is a thick, porous, and irregular layer of material, likely bacterial biofilm or mineral deposits.